SEOUL NATIONAL UNIVERSITY
MONTE CARLO LABORATORY

Evaluation of the Kinetic Characteristics of a Soluble Boron-Free BANDI Core for Main Steam Line Break Accident Analysis

Korea Nuclear Society Spring Meeting

Jeju, Korea, May 8th, 2026

Ikje Noh and Hyung Jin Shim

Monte Carlo Laboratory

Department of Energy Systems Engineering, Seoul National University

Contents

I. Introduction

1. Core Description of BANDI-60 SMR
2. Characteristics of Main Steam Line Break (MSLB) Accidents In Soluble Boron-Free (SBF) Cores
3. Research Objectives

II. Neutronic Analysis Code and Conditions

1. Analysis Code: PRAGMA
2. Scope and Conditions

III. Evaluation Results of the Kinetic Characteristics

1. Post-Trip: Return to Power (RTP) Analysis
2. Pre-Trip: Departure from Nucleate Boiling Ratio (DNBR) Analysis

IV. Conclusion

I. Introduction

1. Core Description of BANDI-60 SMR
2. Characteristics of MSLB Accidents in SBF Cores
3. Research Objectives

1. Core Description of BANDI-60 SMR (1/4)

- Many SMRs are based on a proven pressurized water reactors (PWRs) technology with innovative design features such as passive safety systems and elimination of soluble boron in the reactor coolant system.

- Advantages of adopting soluble boron-free (SBF) Operation [1]:
  ① Reduction in the size of nuclear power plants by simplifying the chemical volume control system
  ② Decrease in the amount of liquid radioactive waste
  ③ Prevention of corrosion caused by boric acid
  ④ Improvement in the inherent safety by a large negative moderator temperature coefficient (MTC)

- Recently, several SBF cores have been under active development domestically, most notably the innovative SMR (i-SMR). In parallel, KEPCO Engineering & Construction (KEPCO E&C) has been independently developing the BANDI-60 SMR, which serves as the target core of this study.

BANDI-60 SMR [2] | KEPCO E&C

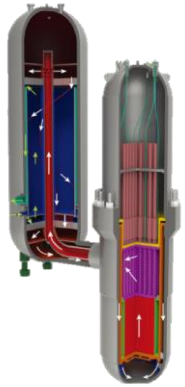

- 200 MWth/60 MWe Power
- 52 FAs
- In-vessel CRDM
- Soluble boron-free
- Single-batch core design

[1] Mart, J., Klein, A., Soldatov, A., 2014. Feasibility study of a soluble boron-free small modular integral pressurized water reactor. Nucl. Technol. 188(1), 8-19.
[2] KEPCO Engineering & Construction. Business/RGD/Nuclear Power/SMR>BANDI. KEPCO E&C Official Website. [Online]. Available: https://www.kepco-enc.com. [Accessed: Mar. 30, 2026].

1. Core Description of BANDI-60 SMR (2/4)

- Design parameters of BANDI-60 SMR core [1]

Parameters	Value
Reactor type	PWR
Coolant and moderator material	Light water
Power (thermal / electrical)	200 MWt / 60 MWe
Primary System pressure	15.51 MPa
Number of FAs	52
FA type	Westinghouse 17 × 17
Uranium enrichment	4.95 wt.%
Fuel material	UO_2
Cladding material	Zircaloy-4
FA pitch	21.5 cm
Pin pitch	1.26 cm
Reactivity control	Pyrex Burnable Absorbers (BA) And Control Rods

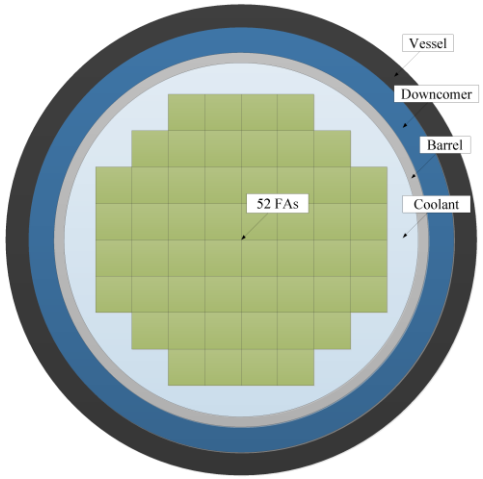

[Radial configurations of BANDI-60 core]

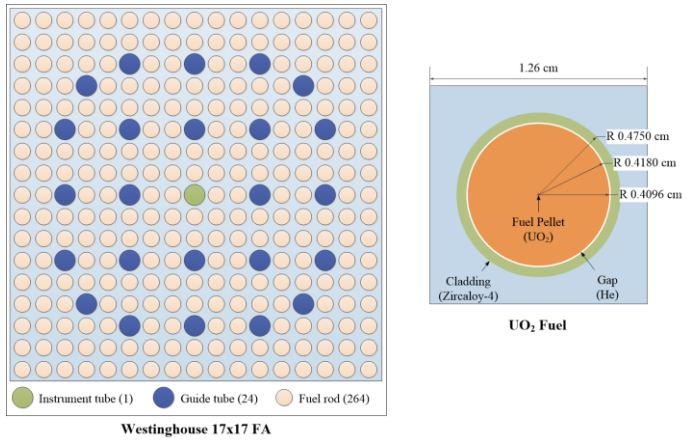

[Radial configurations of WH 17 × 17 FA and UO_2 fuel pellet]

[1] Dokyun Kim, Jong Tae Seo, Hyung Jin Shim,Comparison of BANDI-60 core designs using Pyrex burnable absorber and annular fuel embedding gadolinia wire, Annals of Nuclear Energy, Volume 195, 2024.

1. Core Description of BANDI-60 SMR (3/4)

- Pyrex is the trade name for borosilicate glass consisting of B_2O_3-SiO_2 [1].
  - Pyrex is used to hold down the excess reactivity and achieve the long cycle length of the SBF SMR core design [2,3].
- The Pyrex FA is loaded with 24 Pyrex BAs instead of fuel pins, the loading pattern of which is decided according to the previous study [3].

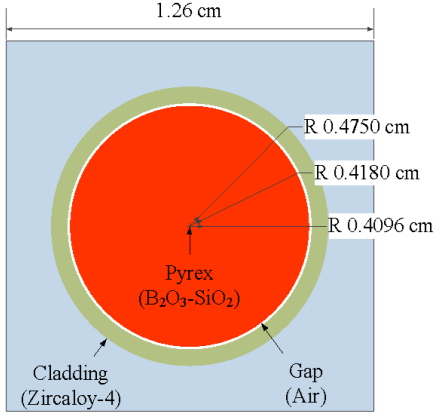

[Radial configuration of Pyrex pin]

- To make smooth radial power distribution, FAs with a high concentration of B_2O_3 are loaded in the center of the core and FAs with a low concentration of B_2O_3 are loaded in the periphery.

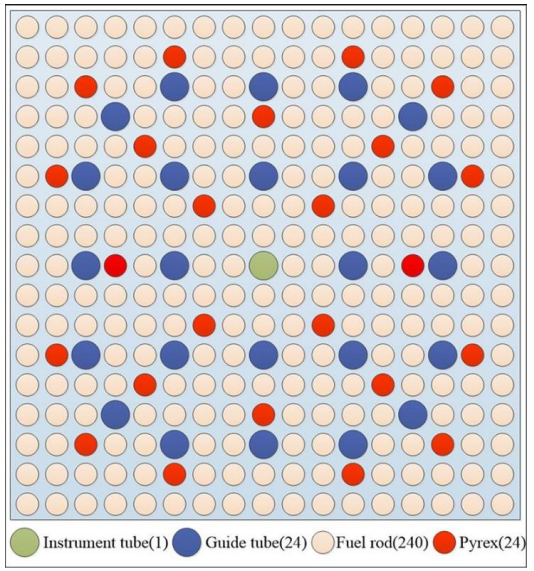

[Radial configuration of Pyrex-loaded FA]

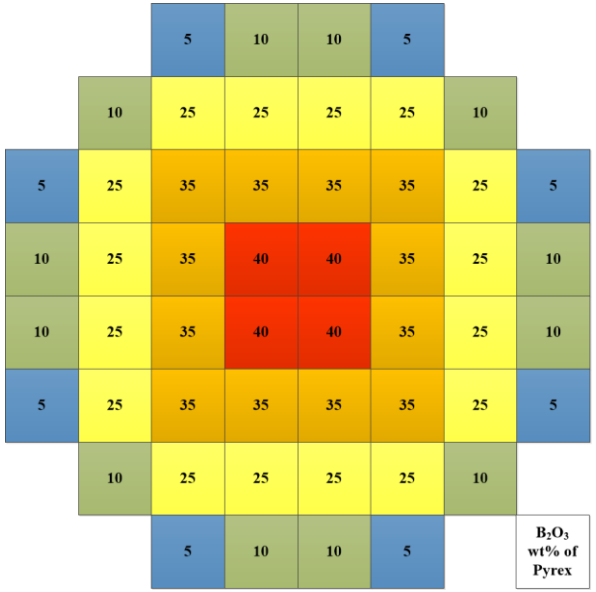

[Loading pattern]

[1] Galahom, A. Abdelghafar. "Study of the possibility of using Europium and Pyrex alloy as burnable absorber in PWR" Annals of Nuclear Energy, 110, 2017.
[2] Kim, Jinsun, et al. "Use of solid pyrex rod for conceptual soluble boron free SMR." Transactions of the American Nuclear Society 115, 2016.
[3] KEPCO E&F, Development of Boron Free Operational Reactor System Design and Material Selection Technology, 2018.

1. Core Description of BANDI-60 SMR (4/4)

- Design of Control Element Assemblies (CEAs)
  - Control rod
    - Material: B_4C
    - Control rods are inserted at 24 guide tube locations.
  - Composition of CEAs
    - Regulating CEA (18): Excess reactivity control
    - Shutdown CEA (22): Reactor shutdown
- The location of CEAs was determined to provide sufficient control rod worth for changes in the core state and maintain the criticality of SBF operation[1, 2].
- CEA Operation Procedure (Draft)
  - CEAs insertion sequence: R4 → R3 → R2 → R1
  - The overlap of CEA bank is set to 20cm, corresponding to 10% of the effective core height (200cm).

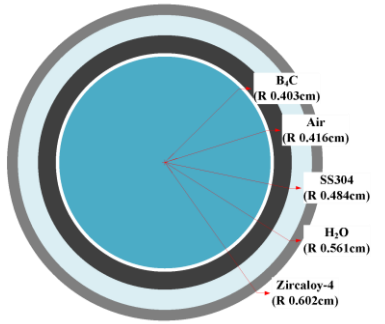

[Radial configuration of control rod]

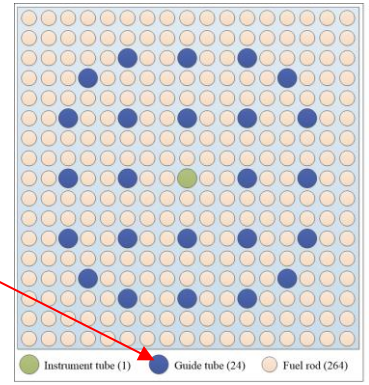

[Radial configuration of FA]

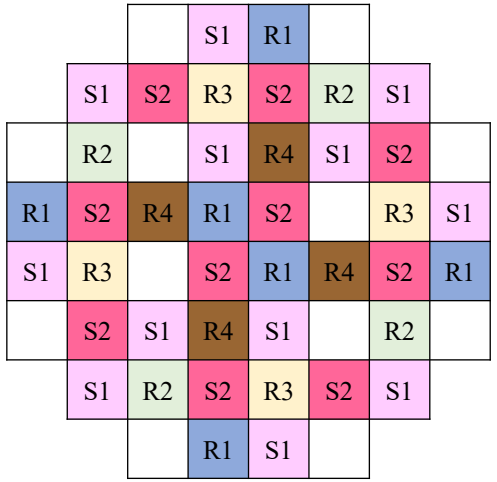

[Configuration of CEAs]

Type	Number of CEAs	Role
R4	4	Regulating
R3	4	
R2	4	
R1	6	
S2	10	Shutdown
S1	12	
Total	40	-

[Information of CEAs]

[1] Kim, I.H., et al., Development of BANDI-60S for a Floating Nuclear Power Plant. Transactions of the Korean Nuclear Society Autumn Meeting, Goyang, Korea, 2016.
[2] Dokyun Kim, Advanced Core Design of Soluble Boron Free Small Modular Reactor for Marine Applications, Master thesis, Seoul National University, 2021.

2. Characteristics of MSLB Accidents in SBF Cores (1/2)

- **Inherent Safety vs. Overcooling Risk:** SBF cores feature a large negative MTC. While it ensures inherent safety during heat-up transients, it acts as a vulnerability during accidents involving an increase in heat removal by the secondary system, due to a massive positive reactivity insertion.

- MSLB Accident Mechanism
  - Steam Line Break

  → Excessive Energy Removal and RCS Cooldown

  → Feedback from Moderator and Fuel Temperature

  → Reactivity Increase

- Two Perspectives in MSLB Safety Analysis

1. [Post-Trip] Return to Power (Re-Criticality)
2. [Pre-Trip] DNBR (Fuel Damage)

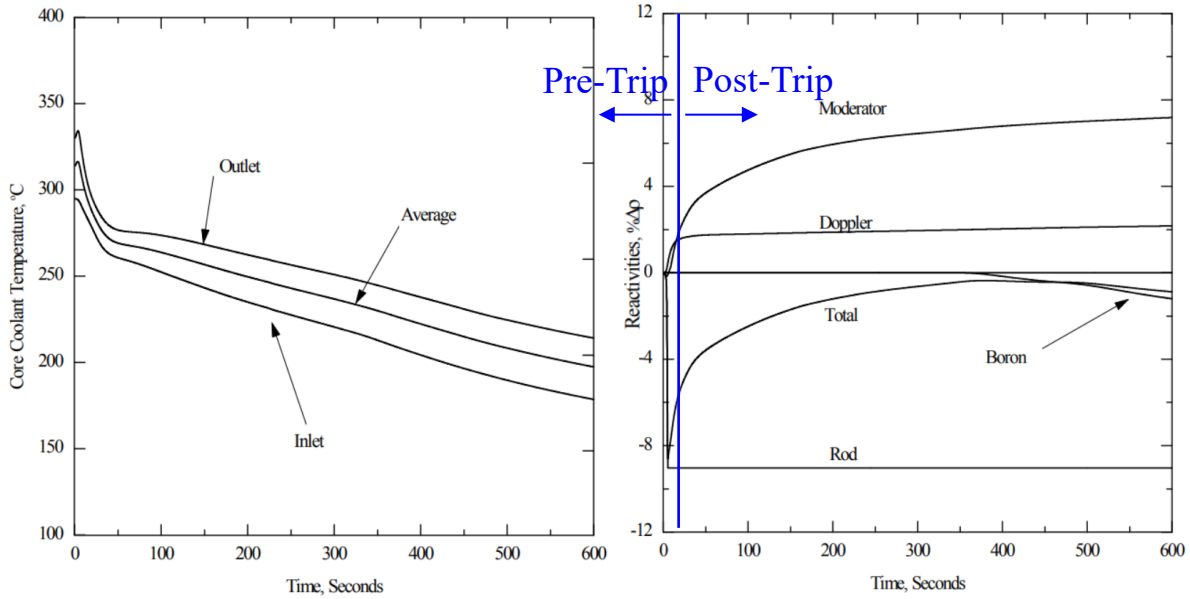

[Full-Power Large Steam Line Break with Concurrent LOOP: Reactivity and Core Coolant Temperature vs. Time at APR1400[1]]

[1] Korea Electric Power Corporation (KEPCO) and Korea Hydro & Nuclear Power Co., Ltd. (KHNP), APR1400 Design Control Document Tier 2, Chapter 15: Transient and Accident Analyses, APR1400-K-X-FS-14002-NP, Rev. 3, 2018.

2. Characteristics of MSLB Accidents in SBF Cores (2/2)

- Comparison of MTC and CEA Worth between APR1400 and SBF BANDI Core
  - While the APR1400 is bounded at EOC due to a highly negative MTC, the BANDI core requires a detailed analysis across the burnup due to significant variations in multiple parameters.

-		APR1400[1]			BANDI		
		BOC	EOC	Difference (EOC – BOC)	BOC	EOC	Difference (EOC – BOC)
Initial Condition		HFP, Eq. Xe., Criticality achieved via CBC			HFP, Eq. Xe., Criticality achieved via CRP		
		ARO, 817 ppm	ARO, 10 ppm	-	CRP, 180 cm	CRP, 0 cm	-
MTC [pcm/K]		-17.1	-43.4	**-26.3**	-91.2	-119.6	**-28.4**
Axial Offset (AO)[1)]		-0.08	0.01	**0.09**	-0.26	0.18	**0.44**
CEA Worth [%Δρ]	Total[2)]	14.5	16.7	2.2	25.1	29.0	3.9
	Bite (Pre-inserted)	-	-	-	2.3	-	-2.3
	Stuck CEA	4.9[3)]	5.7	0.8	5.9	7.5	1.5
	SCRAM[4)]	9.6	11.0	**1.4**	16.9	21.5	**4.7**

1) For the APR1400, the AO, defined as $(P_{top} - P_{bot})/(P_{top} + P_{bot})$, is based on the first cycle core.
2) $\Delta\rho_{\text{Total}} = \rho_{\text{HFP, ARO}} - \rho_{\text{HZP, ARI}}$ (including the power defect from HFP to HZP)
3) This value was estimated by assuming the same ratio of N-1 to total CEA worth as observed at EOC (data not provided).
4) $\Delta\rho_{\text{SCRAM}} = \rho_{\text{Initial Condition}} - \rho_{\text{HZP,N-1}} = \Delta\rho_{\text{Total}} - \Delta\rho_{\text{Bite}} - \Delta\rho_{\text{Stuck CEA}}$ (Uncertainties are not accounted for in this table.)

[1] Korea Electric Power Corporation (KEPCO) and Korea Hydro & Nuclear Power Co., Ltd. (KHNP), "APR1400 Design Control Document Tier 2, Chapter 4: Reactor," APR1400-K-X-FS-14002-NP, Rev. 3, 2018.

3. Research Objectives (1/1)

- Main Objective
  - Evaluation of the kinetic characteristics during the MSLB accident through high-fidelity neutronic analysis of the SBF BANDI-60 core.
- Specific Objectives
  - Identification of Unique Kinetic Characteristics in MSLB Accident Analysis of SBF Core
  - Preliminary Quantification of Safety Margins for BANDI Core under MSLB Accident

II. Neutronic Analysis Code and Conditions

1. Analysis Code: PRAGMA
2. Scope and Conditions

1. Analysis Code: PRAGMA (1/1)

- Power Reactor Analysis using GPU-based Monte Carlo Algorithm (PRAGMA)*

* Funded by KHNP through K-CLOUD project

  - Unlike conventional PWRs, SBF cores lack historical operating data, which imposes excessive conservatism and uncertainty penalties in safety analyses.
  - To resolve such excessive conservatism, a first-principles-based, continuous-energy Monte Carlo approach can be directly utilized, or its high-fidelity results can potentially serve as reference data substituting for the actual measurements.
  - However, traditional CPU-based Monte Carlo codes require immense computational resources, tightly limiting their application in practical safety analyses.
  - In this context, PRAGMA enables these high-fidelity Monte Carlo simulations within a practical time frame, utilizing a small-scale cluster equipped with consumer-grade GPUs[1].

[1] Namjae Choi, Kyung Min Kim, Han Gyu Joo, Initial Development of PRAGMA – A GPU-Based Continuous Energy Monte Carlo Code for Practical Applications. Transactions of the Korean Nuclear Society Autumn Meeting, Goyang, Korea, 2019.

2. Scope and Conditions (1/4)

- Scope
  - Base Depletion: Generate material compositions for each burnup step under normal operating conditions.
  - Restart Calculation: Evaluate varied parameters using material compositions generated during Base Depletion.

  * The kinetic characteristics were evaluated via static k-eigenvalue calculations at each restart condition.

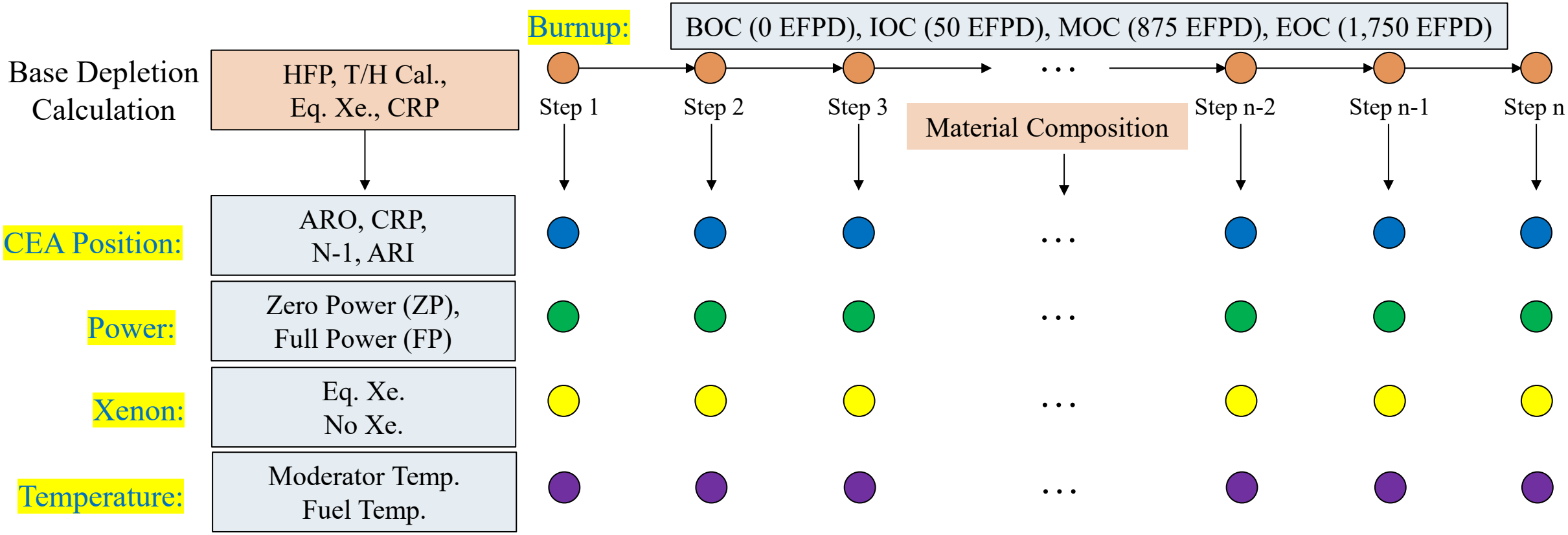

2. Scope and Conditions (2/4)

- Base Depletion Calculation

Cross-section	ENDF/B-VII.1
# of Particles per Cycle	8,000,000
# of Active Cycles / # of Inactive Cycles	50 / 30
T/H Feedback	Applied
Inlet Moderator Temperature	563.15K (290°C)
Equilibrium Xenon (Eq. Xe.)	Applied
Critical Rod Position (CRP) Search Algorithm	Applied
CEA Depletion	Applied

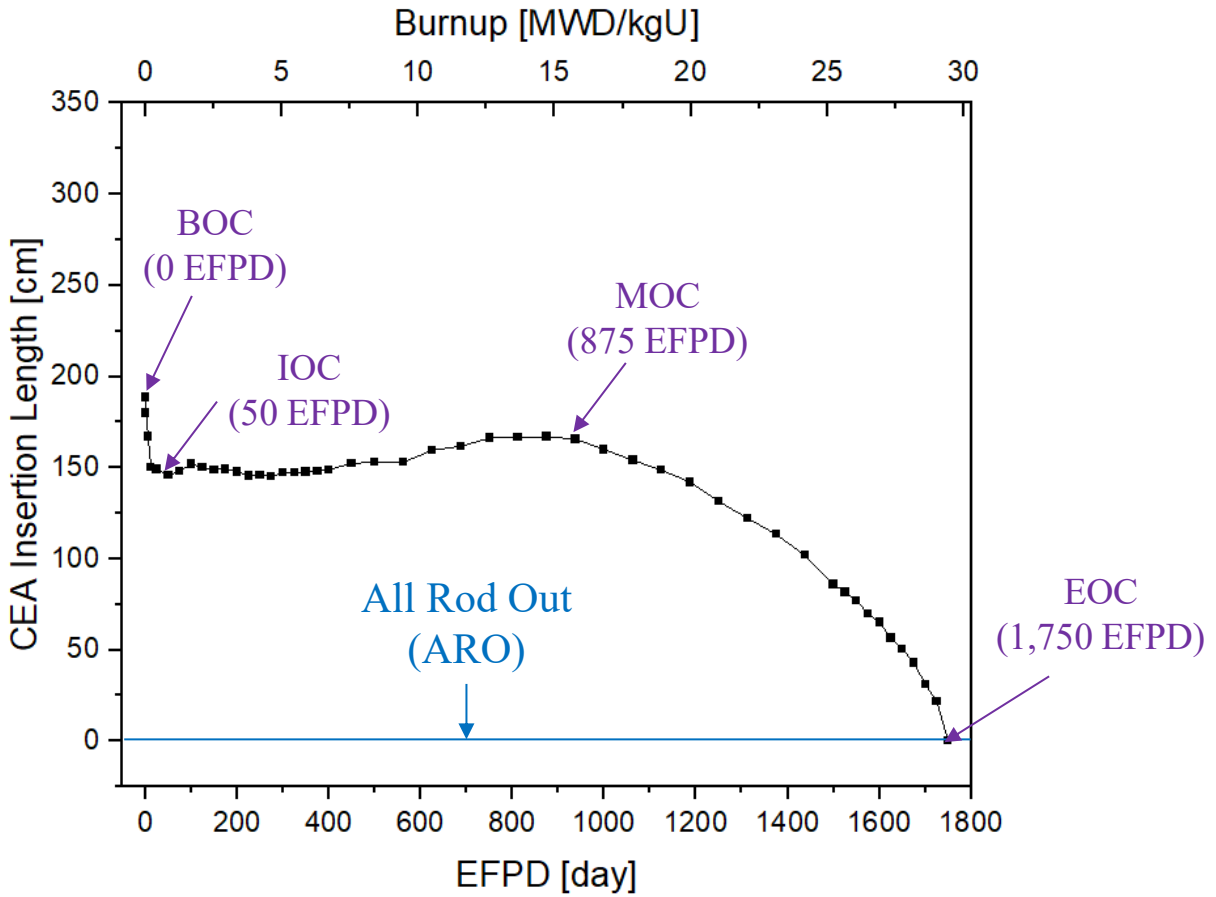

[CEA Insertion Length for Criticality vs. EFPD]

* The design cycle length is approximately 1,750 EFPD (~4.8 EFPY).
* The standard deviation of k_{eff} is maintained within 3–5 pcm across all burnup steps.
* The eigenvalue calculation at EOC takes approximately 10 minutes using 8 NVIDIA RTX A5000 GPUs.

2. Scope and Conditions (3/4)

- Critical Rod Position (CRP) under Various Conditions

  * The CRP plays the equivalent role of the Critical Boron Concentration (CBC) in conventional large PWRs.

Burnup Step	CEA Insertion Length [cm]			
	HFP		HZP	
	Eq. Xe.	No Xe.	Eq. Xe.	No Xe.
BOC (0 EFPD)	180	308	340	477
IOC (50 EFPD)	146	284	319	408
MOC (875 EFPD)	167	304	327	438
EOC (1,750 EFPD)	0	86	116	249

- **Eq. Xe. Condition**: The Xe number density is fixed to the value of the normal operating condition (HFP, CRP, Eq. Xe.) at each burnup step, regardless of variations in power, CEA position and temperatures.
- **No Xe. Condition**: Xe-135 and I-135 isotopes completely removed.

2. Scope and Conditions (4/4)

- ARI w/ Most Reactive CEA Stuck Condition (N-1)
  - Using the equation below, the CEA with the maximum shutdown reactivity worth was identified, and the scenario in which this specific CEA is stuck out was selected as the N-1 condition.

$$\Delta\rho = \rho_{\mathrm{N-1,CEA}_i} - \rho_{\mathrm{ARI}}$$

  - The B7 CEA exhibits the highest reactivity worth across all conditions.

* Details in Appendix A.1: N-1 Condition Search Results

-	Most Reactive CEA	2nd Most Reactive CEA
CEA Index	B7	C6

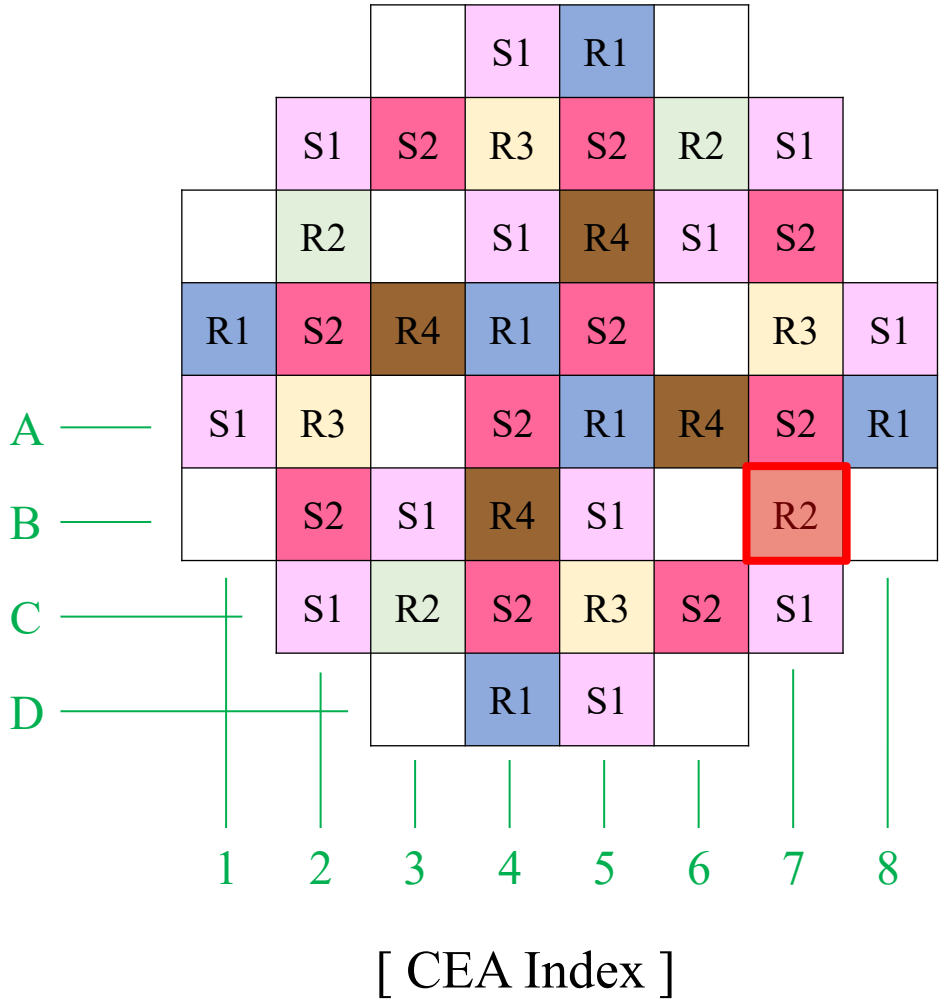

[CEA Index]

III. Evaluation Results of the Kinetic Characteristics

1. Post-Trip: RTP Analysis
2. Pre-Trip: DNBR Analysis

1. Post-Trip: RTP Analysis (1/4)

- Reactivity Behavior during Cooldown * BOC, No Xe. and Constant Nominal RCS Pressure (15.51 MPa) Conditions
  - By utilizing the substantial SCRAM worth characteristic of SBF cores, the need for a Post-Trip analysis during an MSLB can be completely eliminated, provided that the CEAs alone provide an adequate Shutdown Margin (SDM) at Cold Zero Power (CZP) under the most conservative conditions.

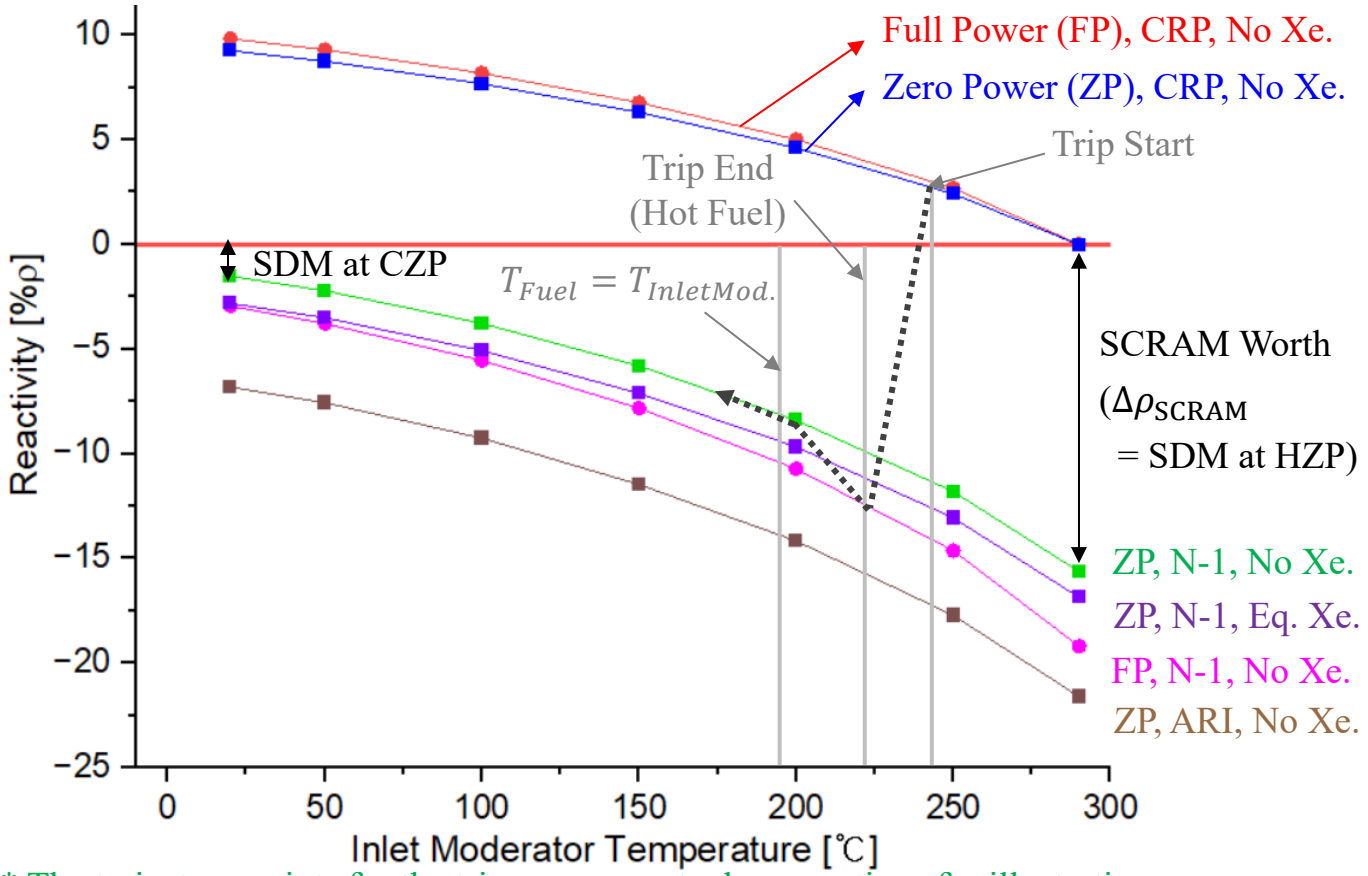

* The trajectory points for the trip are conceptual assumptions for illustrative purposes.

Post-Trip Reactivity Components [%Δρ]	Inlet Mod. Temp.	
	290℃	20℃
$\Delta\rho_{SCRAM} = \rho_{CRP} - \rho_{N-1}$	15.64	11.35
$\Delta\rho_{StuckCEAworth} = \rho_{N-1} - \rho_{ARI}$	5.98	5.30
$\Delta\rho_{XenonDefect} = \rho_{NoXe.} - \rho_{Eq.Xe.}$	1.23	1.30
$\Delta\rho_{PowerDefect} = \rho_{ZP} - \rho_{FP}$ [1)]	3.57	1.42

※ In this study, the SCRAM worth($\Delta\rho_{SCRAM}$) is defined as the value evaluated under HZP (N-1) conditions, including the power defect. Furthermore, temperature-induced variations in the SCRAM worth and xenon defect are accounted for within the total reactivity inserted during the cooldown process.

1) $\rho_{FP,N-1}$ is calculated with fuel and moderator temperatures fixed at the FP, CRP

1. Post-Trip: RTP Analysis (2/4)

▪ SDM Analysis at CZP (N-1) Condition

- The BOC under No Xenon condition is identified as the most limiting case across all conditions due to its lowest available SCRAM worth and the absence of decay heat to mitigate the overcooling.
- Because the current CEA design yields an insufficient final SDM of 0.29%Δρ, it is necessary to increase the B-10 enrichment of the shutdown CEAs or adopt an additional shutdown mechanism.

Reactivity Components [%Δρ]	BOC		IOC		MOC		EOC	
	Eq. Xe.	No Xe.	Eq. Xe.	No Xe.	Eq. Xe.	No Xe.	Eq. Xe.	No Xe.
① SDM at HZP (N-1)[1)]	16.85	15.63	17.37	16.20	18.42	17.13	21.55	20.06
② SDM at CZP (N-1)[2,3)]	2.80	1.85	3.43	2.53	5.35	4.39	8.16	6.92
③ SCRAM Worth at HZP w/ Uncertainty [4)] (①×0.9)	15.16	14.06	15.64	14.58	16.58	15.42	19.39	18.06
④ Inserted Reactivity due to Cooldown (HZP→CZP) (①-②)	14.04	13.78	13.94	13.67	13.06	12.74	13.39	13.15
⑤ Final SDM[5)] (③-④)	1.12	**0.29**	1.70	0.91	3.51	2.68	6.01	4.91

1) SDM at HZP (N-1) is equivalent to the available SCRAM worth at normal operating conditions
2) CZP is defined at 20°C, 0.10 MPa (1 atm). Assuming a constant nominal RCS pressure (15.51 MPa) during a cooldown yields a more severe SDM of 1.51%Δρ—rather than the 1.85%Δρ evaluated at 0.1 MPa—under BOC (CZP and No Xe.) conditions, which is physically unrealistic.
3) In this table, decay heat was neglected. However, accounting for decay heat increases the SDM at EOC (CZP, No Xe.) increasing from 6.92%Δρ to 7.00 %Δρ.
4) An uncertainty of 10% is applied to the SCRAM worth.
5) Uncertainty for the final SDM is not accounted for; applying this would further reduce the final SDM.

1. Post-Trip: RTP Analysis (3/4)

- Impact of CEA Depletion on SDM
  - Adopting a 2-cycle CEA lifetime (9.6 EFPY, comparable to the ~10-year design life of APR1400 CEAs) results in a SCRAM worth penalty of 0.08%Δρ at the most conservative condition (Cycle 2 BOC).
  - This level of SCRAM worth penalty is sufficiently small, having a negligible impact on the SDM.

Cycle # (CEA Depletion Period)	SCRAM worth at HZP and No Xe. Conditions (Difference) [%Δρ]		
	BOC (0 EFPD)	MOC (875 EFPD)	EOC (1,750 EFPD)
Fresh CEA (w/o CEA Depletion)	-	17.17	20.12
Cycle 1 (0~4.8 EFPY)	15.63 (-)	17.13 (-0.04)	20.06 (-0.06)
Cycle 2 (4.8~9.6 EFPY)	15.55 (-0.08)	17.05 (-0.12)	20.03 (-0.09)[1)]
Cycle 3 (9.6~14.4 EFPY)	15.46 (-0.17)	16.92 (-0.25)	19.96 (-0.16)[1)]

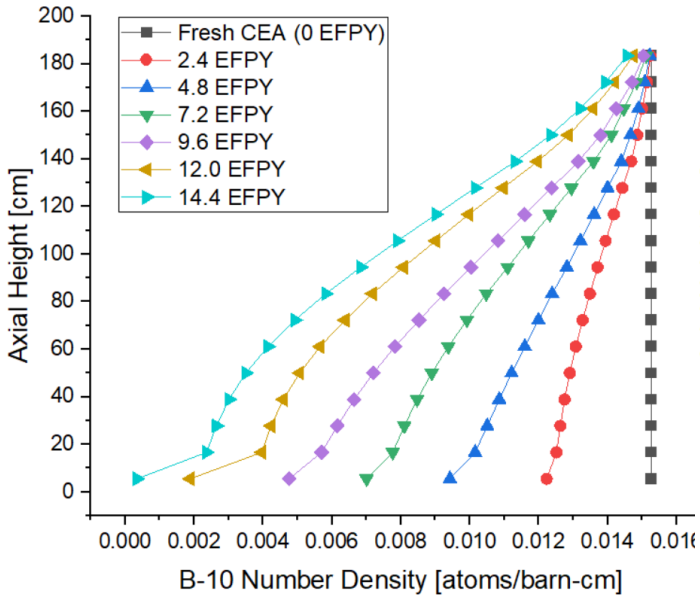

[B-10 Number Density in R4 Bank]

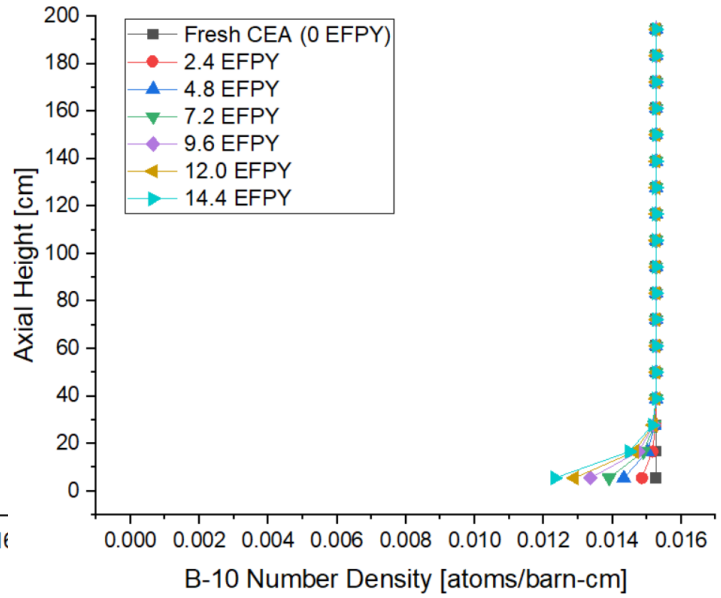

[B-10 Number Density in S2 Bank]

1) The top-skewed axial power distribution at EOC mitigates the penalty of CEA bottom depletion.

1. Post-Trip: RTP Analysis (4/4)

- Application of Enriched B_4C in Shutdown CEAs
  - Enriched B_4C was strategically applied exclusively to shutdown CEAs—rather than to all CEAs including regulating CEAs—to avoid the prohibitive costs, excessive local power peaking during normal operation, and reduced safety margins during a Rod Ejection Accident (REA).
  - Even when applying a 500pcm uncertainty to the final SDM, all enriched B_4C cases secure sufficient margin.
  - However, the economic feasibility of adopting enriched B_4C must be evaluated, given that enriched B_4C (96 w/o B-10) is approximately 100 times more expensive than natural B_4C [1].

B-10 Enrichment of Shutdown CEA [a/o]		19.9	30.0	50.0	70.0	90.0
Density[1] [g/cm^3]		1.76	1.75	1.72	1.70	1.67
Reactivity Components at BOC (No Xe.) [%Δρ]	SCRAM Worth at HZP w/ Uncertainty[2]	14.06	14.75	15.37	15.76	16.08
	Inserted Reactivity due to Cooldown	13.78	14.12	14.40	14.58	14.74
	Final SDM at CZP	0.29	**0.63**	**0.98**	**1.18**	**1.34**

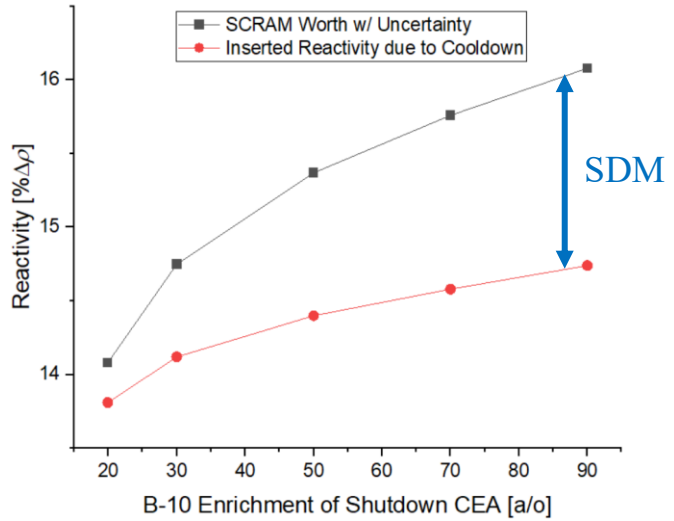

1) The applied B_4C pellet density is 70% of the theoretical density (TD), assuming a constant pellet volume across all B-10 enrichments.
2) Applying enriched B_4C to the Shutdown CEAs changes the most reactive stuck CEA from B7 (R2 Bank) to C6 (S2 Bank) under the N-1 condition.

[1] J. H. Prosser *et al.*, "First-Principles Cost Estimation of a Sodium Fast Reactor Nuclear Plant," INL/RPT-23-74316 Rev. 1, Idaho National Laboratory (2024).

2. Pre-Trip: DNBR Analysis (1/12)

- Scenario[1)] and Analysis Methodology

Normal Operation (HFP, 102% Power)

MSLB Initiation

RCS Overcooling and Power Excursion

Trip Setpoint Reached (121% Power)

Trip Delay Time (0.65sec) [1)]

Reactor Trip & RCP Coastdown

MDNBR

PRAGMA
- Reactivity Coefficients (MTC, MDC, FTC) * Appnedix 2
- Kinetic Parameter ($\beta_{eff,i}, \lambda_i, \Lambda$) * Appnedix 3
- SCRAM Worth vs. CEA position * Appnedix 4
- Power Distribution * Appnedix 4
- Decay Heat * Appnedix 5

Point Kinetics Model
- Power & Reactivity vs. Time
- Average Moderator & Fuel Temp vs. Time
- RCS Pressure vs. Time
- Core Flow Rate vs. Time

External Input Data
- CEA Position vs. Time
- Core Inlet Temp. vs. Time
- RCP Coastdown Flow Rate vs. Time
- IAPWS-97 Steam Table

2006 CHF Groeneveld Look Up Table
- DNBR vs. time

[1] Korea Electric Power Corporation (KEPCO) and Korea Hydro & Nuclear Power Co., Ltd. (KHNP), "APR1400 Design Control Document Tier 2, Chapter 15: Transient and Accident Analyses," APR1400-K-X-FS-14002-NP, Rev. 3, 2018.

2. Pre-Trip: DNBR Analysis (2/12)

- SCRAM Worth vs. Time * HFP and CRP Conditions
  - For this analysis, the limiting APR1400 acceptance curve [1] was applied as the time-dependent CEA position.
  - The SCRAM worth was evaluated assuming CEA insertion from the CRP to the ARI (N-1) condition

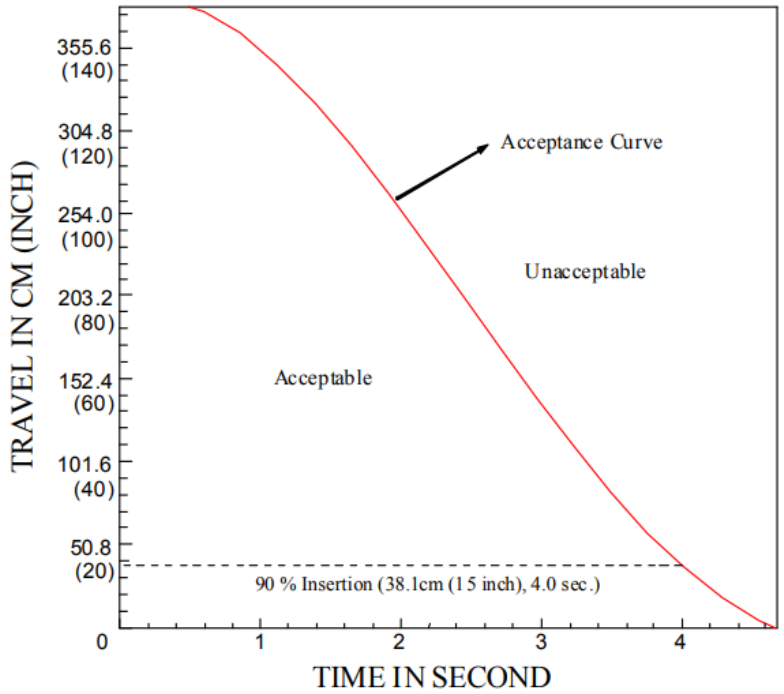

[CEA Position Requirements during Reactor Scram for APR1400]

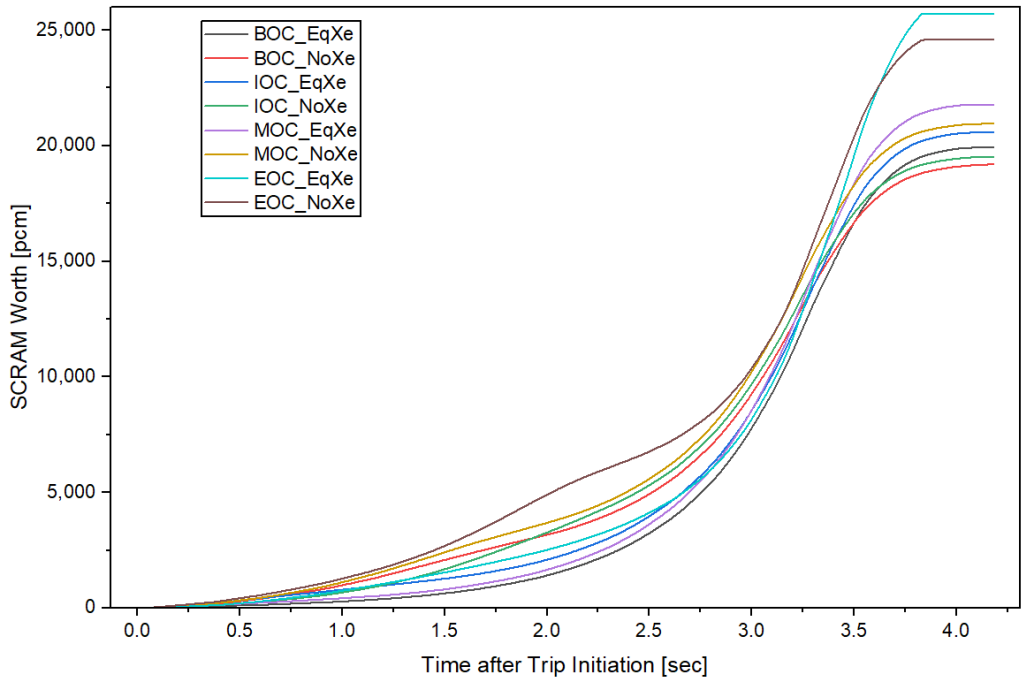

[SCRAM Worth vs. Time from CRP to N-1 Condition]

[1] Korea Electric Power Corporation (KEPCO) and Korea Hydro & Nuclear Power Co., Ltd. (KHNP), "APR1400 Design Control Document Tier 2, Chapter 4: Reactor," APR1400-K-X-FS-14002-NP, Rev. 3, 2018.

2. Pre-Trip: DNBR Analysis (3/12)

- Inlet Moderator Temperature Change Rate
  - Considering the short time scale of the pre-trip analysis for the BANDI core (< 7 sec), the inlet moderator temperature change rate was assumed to be linear. The reference value of the rate (-4.5K/sec) was determined by the most conservative value from the OECD/NEA MSLB Benchmark [1].
  - Asymmetric overcooling is not considered due to the 1-loop design of the BANDI core.

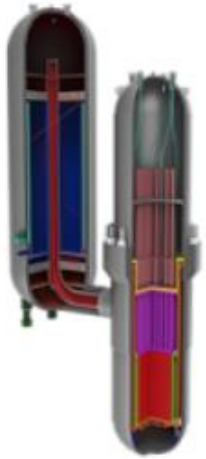

[Schematic View of the BANDI-60]

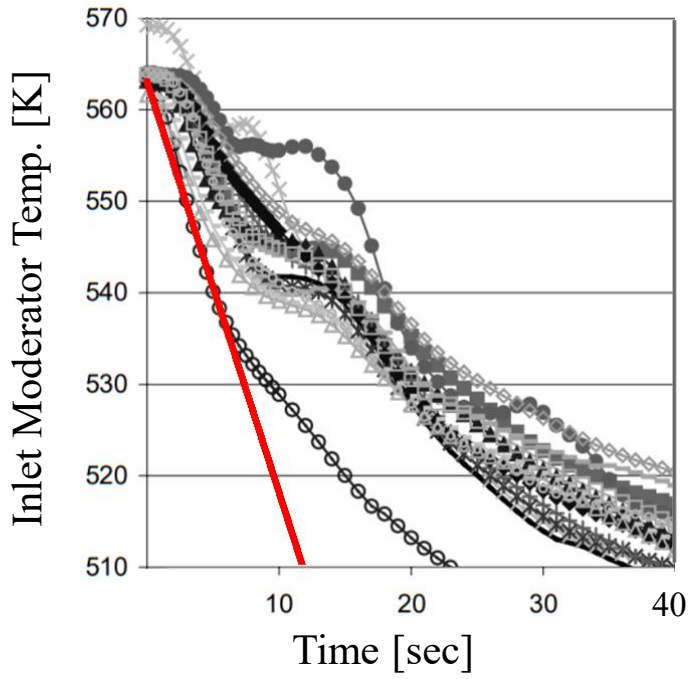

[Broken cold leg temperature of OECD/NEA MSLB Benchmark.]

[1] T. Beam et al., "PWR MSLB Benchmark, Vol. II: Summary Results of Phase I (Point Kinetics)," OECD/NEA, NEA/NSC/DOC(2000)21, 2000.

2. Pre-Trip: DNBR Analysis (4/12)

- RCP Coastdown Curve
  - The Reactor Coolant Pumps (RCPs) of BANDI are driven by canned motors.
  - The BANDI coastdown curve is based on the coastdown data of the SMART reactor [1], which utilizes an identical canned-motor RCP design.
  - This curve was modeled using the equation below, yielding a calculated coastdown coefficient (α) of 0.255.

$$\frac{W(t)}{W_0} = \frac{1}{1 + \alpha \cdot t}$$

where:

$W(t)$: Mass flow rate at time t

α : Coastdown coefficient

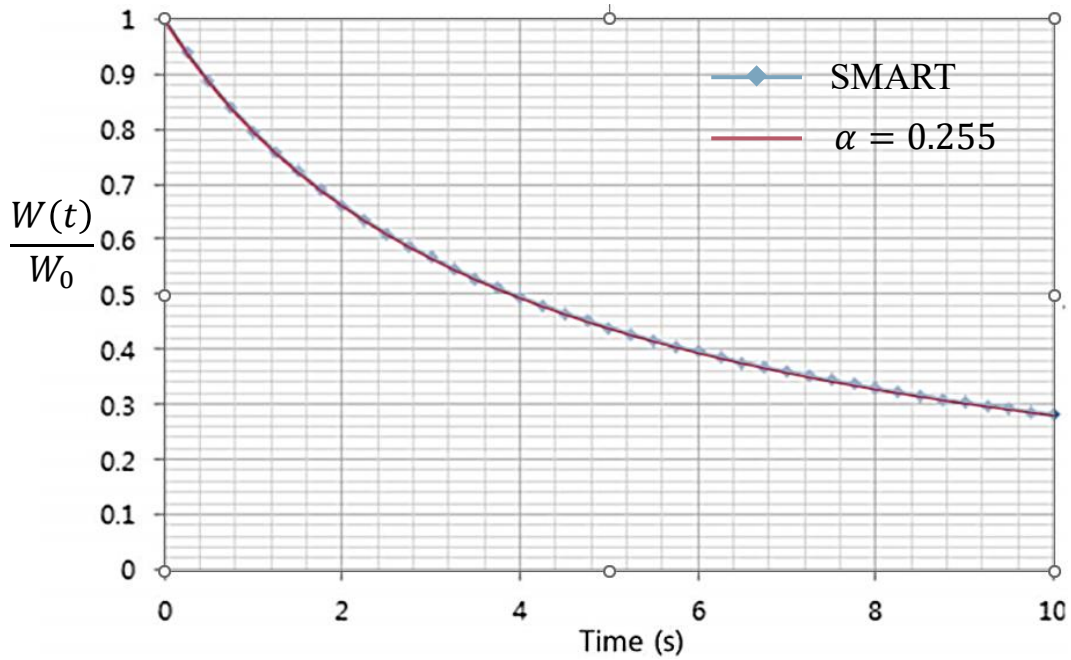

[1] J. Song, " Enhancement and Verification of SMART Reactor Coolant System," Korea Atomic Energy Research Institute, Seoul, South Korea, Tech. Rep. TRKO202000006585, Feb. 2019.

2. Pre-Trip: DNBR Analysis (5/12)

- Uncertainty
  - All uncertainties are deterministically applied in the direction that minimizes the MDNBR.
  - The specific penalty direction (+ or -) for each parameter was individually evaluated to ensure the most limiting MDNBR.

Variables	Uncertainty
SCRAM Worth	-10%
Decay Heat Fraction	-20%
Kinetic Parameters	±5%
MDC	+10%
Cross-Section Component of MTC	±15%
FTC	-15%
Pin-wise Fq	+15%
Critical Heat Flux (CHF)	-15%

2. Pre-Trip: DNBR Analysis (6/12)

- Sensitivity Analysis of Neutronic Parameter
  - To quantitatively evaluate the impact of each kinetic parameter on the MDNBR, the relative sensitivity (S_{rel}) was calculated. It is defined as the fractional change in the MDNBR per 1% increase in the parameter.

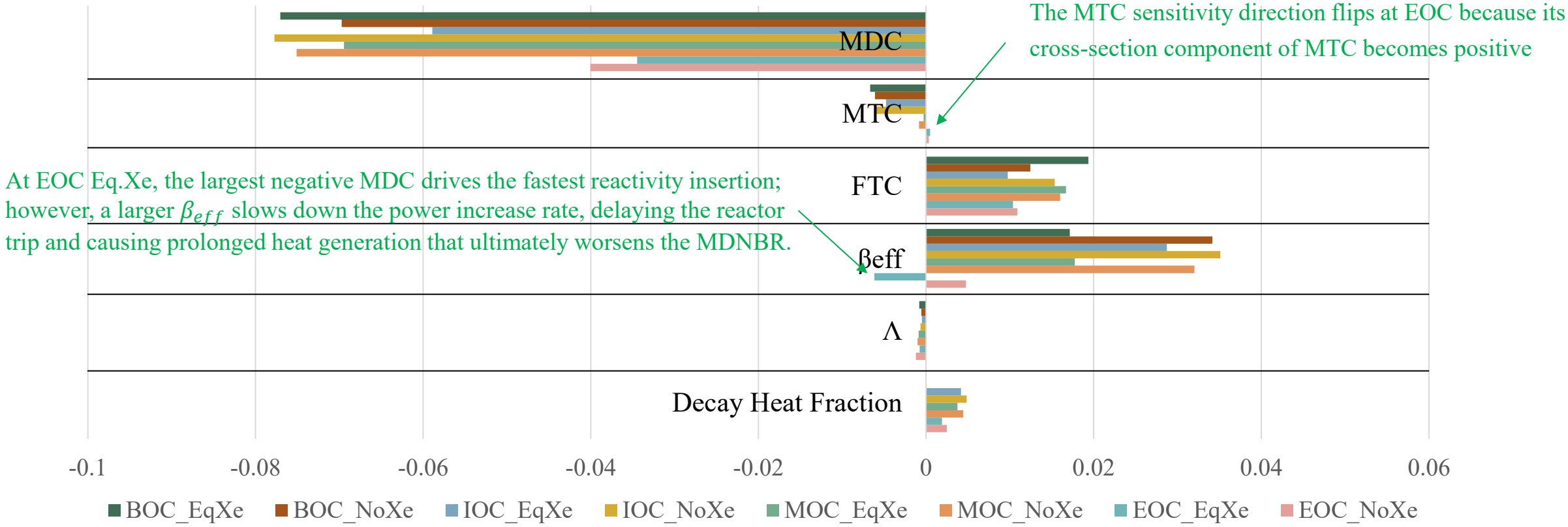

2. Pre-Trip: DNBR Analysis (7/12)

- Sensitivity Analysis of Thermal-Hydraulic and System Parameters
  - The sensitivity analysis results indicate that Thermal-Hydraulic and System parameters exert a more dominant influence on the MDNBR than Neutronic parameters.

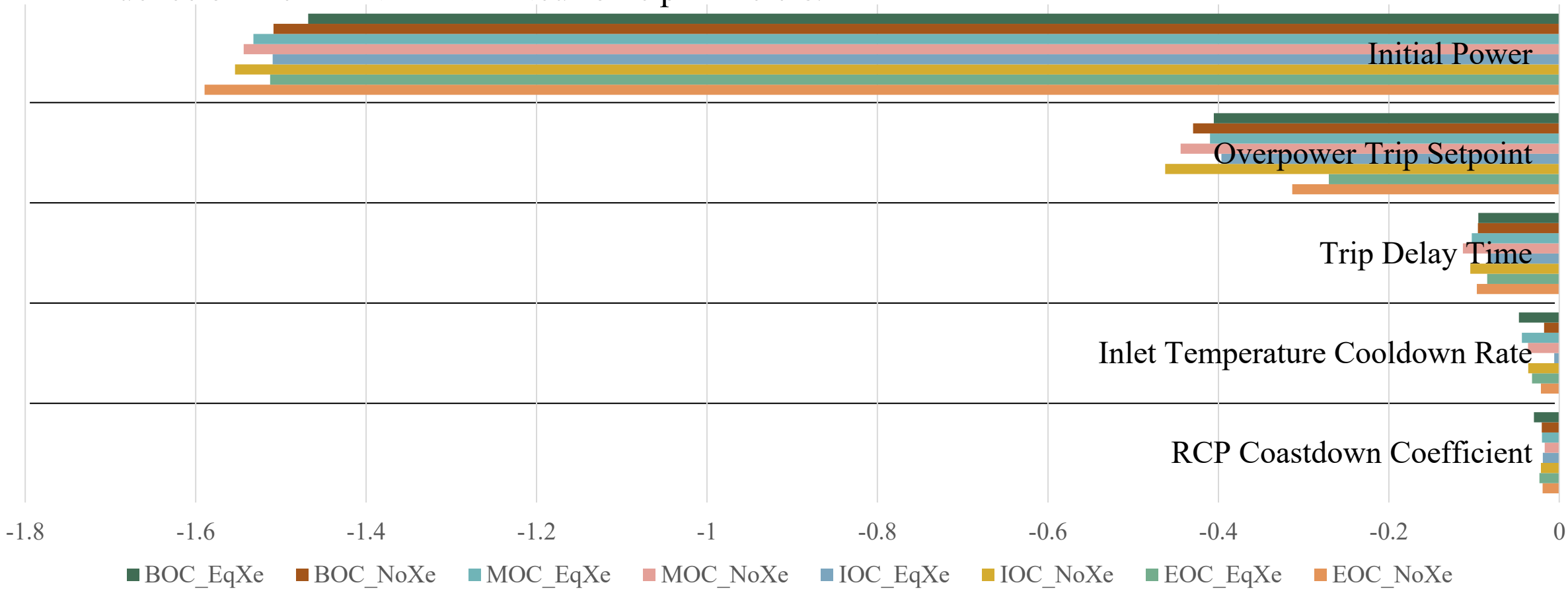

2. Pre-Trip: DNBR Analysis (8/12)

- Verification of Monotonicity in Neutronic Parameter Uncertainties
  - The impact of each neutronic parameter on the MDNBR is strictly monotonic under all conditions.
  - This monotonicity indicates that the worst MDNBR is inevitably found at the two extremes of the uncertainty range.

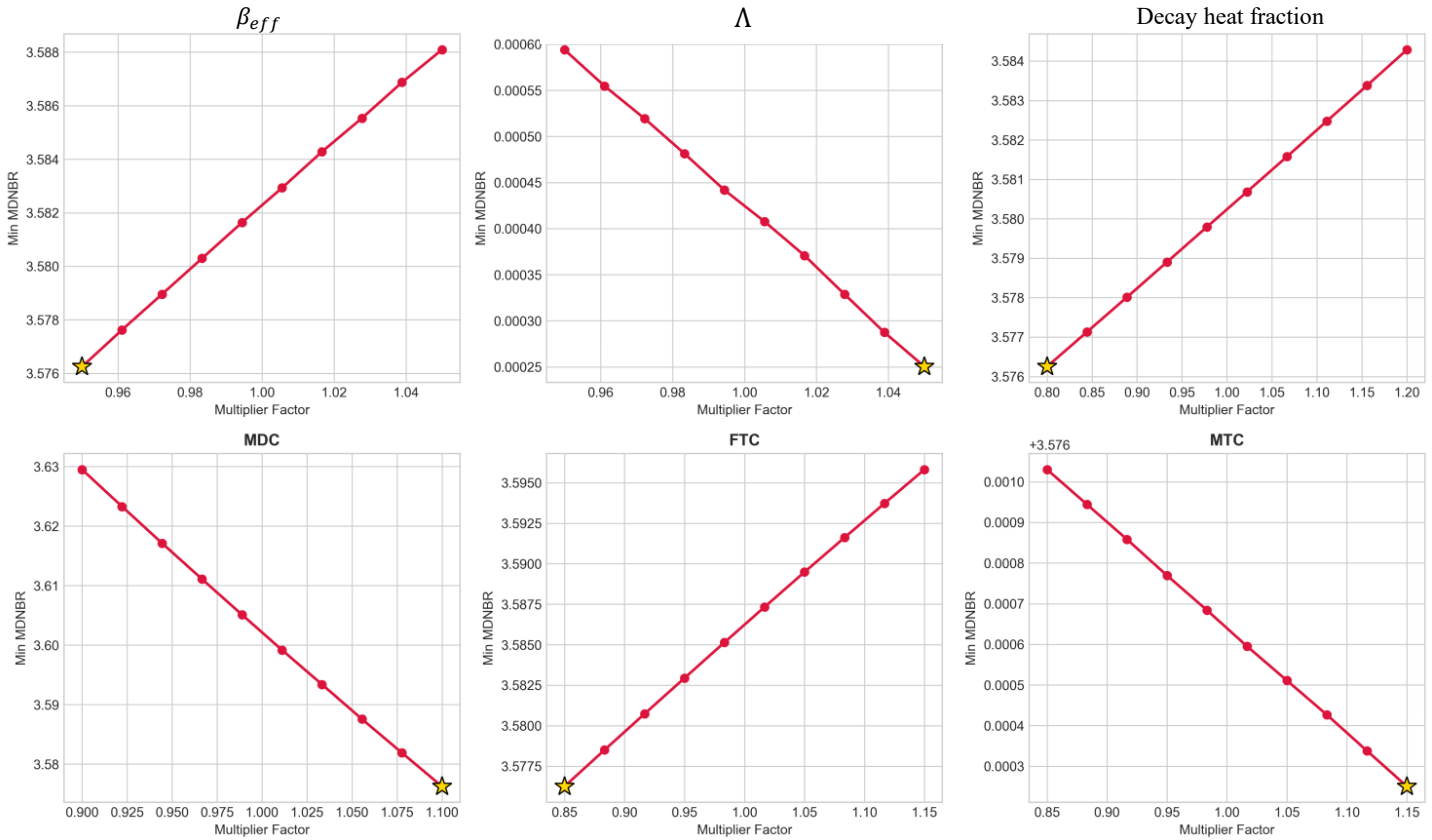

[Impact of Neutronic Parameter on Minimum MDNBR (MOC, NoXe)]

2. Pre-Trip: DNBR Analysis (9/12)

- MDNBR Evaluation * Comprehensive details of the point kinetics feedback model are provided in Appendix A.5.
  - The MOC NoXe scenario exhibits the lowest MDNBR (3.57), which maintains a substantial safety margin against the design limit specifically established as 1.40 for this study.

: Most Limiting Condition

Condition		MDC [pcm/(kg/m^3)]	FTC [pcm/$\sqrt{K}$]	β_{eff} [pcm]	SCRAM Worth [%Δρ]	Axial Offset	Fq at Normal Operation	Time of Trip Start	Time of Peak Power (% Power)	Time of MDNBR (MDNBR Value)
BOC	Eq. Xe.	35.6	-128.1	708	19.9	-0.25	2.46	0.91 sec	1.63 sec (152.2%)	2.47 sec (3.97)
	No Xe.	32.8	-125.3	708	19.2	-0.50	2.64	0.96 sec	1.61 sec (152.0%)	2.09 sec (3.78)
IOC	Eq. Xe.	30.1	-122.1	687	20.6	-0.35	2.19	0.99 sec	1.65 sec (147.7%)	2.06 sec (4.63)
	No Xe.	33.3	-129.9	694	19.5	-0.44	2.50	0.95 sec	1.67 sec (152.4%)	2.18 sec (3.83)
MOC	Eq. Xe.	36.8	-140.7	583	21.8	-0.26	2.15	0.85 sec	1.51 sec (152.2%)	2.05 sec (4.46)
	No Xe.	36.4	-142.6	581	21.0	-0.50	2.69	0.86 sec	1.51 sec (155.5%)	1.91 sec (3.57)
EOC	Eq. Xe.	54.0	-152.3	531	25.7	+0.18	2.30	0.66 sec	1.32 sec (150.2%)	1.86 sec (4.66)
	No Xe.	47.3	-151.1	536	24.6	-0.07	2.46	0.69 sec	1.35 sec (154.2%)	1.69 sec (5.57)

-	APR1400	SMART	SMART100	i-SMR	NuScale	BANDI
Thermal Power [MWth]	3,983	330	365	520	160	200
Average Linear Heat Generation Rate [W/cm]	179	110	120	119	82	80

2. Pre-Trip: DNBR Analysis (10/12)

- DNBR vs. Time

* Detailed results, including core power, RCS pressure, and mass flow rate over time, are provided in Appendix A.6.

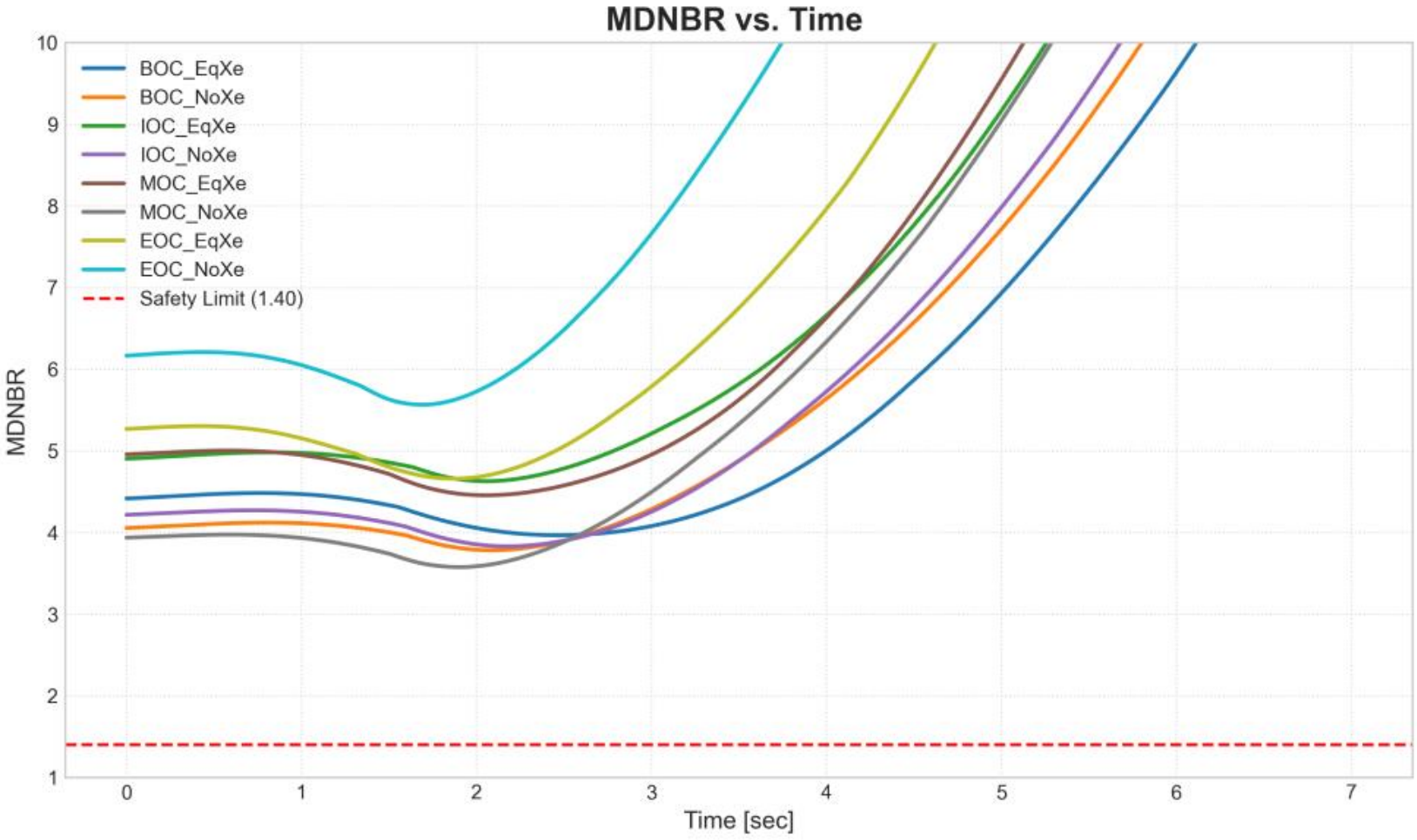

Condition		MDNBR
BOC	Eq. Xe.	3.97
	No Xe.	3.78
IOC	Eq. Xe.	4.63
	No Xe.	3.83
MOC	Eq. Xe.	4.46
	No Xe.	3.57
EOC	Eq. Xe.	4.66
	No Xe.	5.57

2. Pre-Trip: DNBR Analysis (11/12)

- Conservatism in CEA Initial Position
  - In SBF cores, regulating CEA banks are inherently pre-inserted during normal operation to maintain criticality.
  - A trip initiated from the CRP provides a faster initial reactivity insertion rate compared to the ARO condition.
  - Since the CRP varies depending on the burnup and xenon conditions, the CRP-to-ARI transition was initially used to establish a fair baseline for comparison across different burnup steps.
  - Given that the CEA operational strategy is still under development, the ARO-to-ARI scenario must be evaluated to ensure a bounding and conservative safety margin.

Condition		MDNBR (CRP→N-1)	MDNBR (ARO→N-1)	Difference (ARO-CRP)
BOC	Eq. Xe.	3.97	3.85	-0.12
	No Xe.	3.78	3.52	-0.26
IOC	Eq. Xe.	4.63	4.37	-0.26
	No Xe.	3.83	3.63	-0.20
MOC	Eq. Xe.	4.46	4.25	-0.21
	No Xe.	3.57	3.32	-0.25
EOC	Eq. Xe.	4.66		-
	No Xe.	5.57	5.40	-0.17

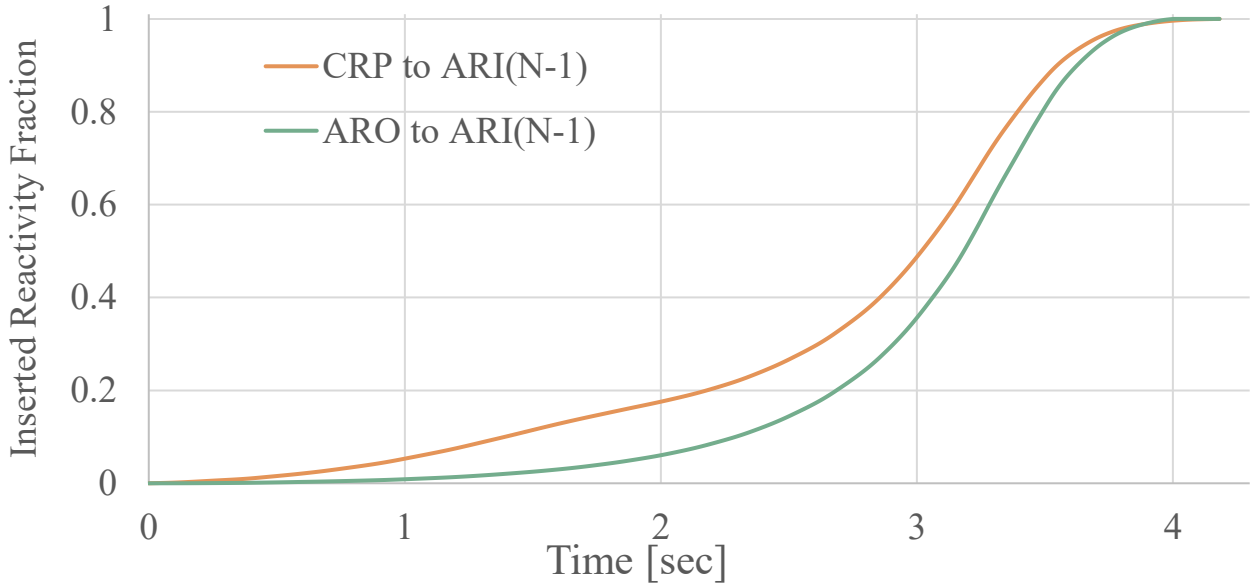

[Comparison of Normalized Scram Reactivity Insertion: CRP vs. ARO (MOC, No Xe)]

2. Pre-Trip: DNBR Analysis (12/12)

- Impact of CEA Depletion on MDNBR
  - In SBF cores, CEAs experience substantial B-10 depletion at the bottom segments compared to conventional boron-controlled cores.
  - This depletion significantly delays the negative reactivity insertion at the early stages of a reactor trip.
  - Therefore, a quantitative evaluation of the impact of B-10 depletion at the CEA tip on the MDNBR is required.
  - Under the current CEA operating strategy, severe B-10 depletion is strictly localized to the R4 regulating bank, while other banks show minimal depletion (e.g., S2 bank); consequently, the overall impact of CEA tip depletion on the MDNBR is marginal.

Condition	MDNBR (No CEA Depletion)	MDNBR (Cycle 1, 2.4 EFPY)	MDNBR (Cycle 2, 7.2 EFPY)	Difference (Cycle 2 – Cycle1)
MOC, No Xe., CRP to ARI	3.575	3.571	3.568	-0.003

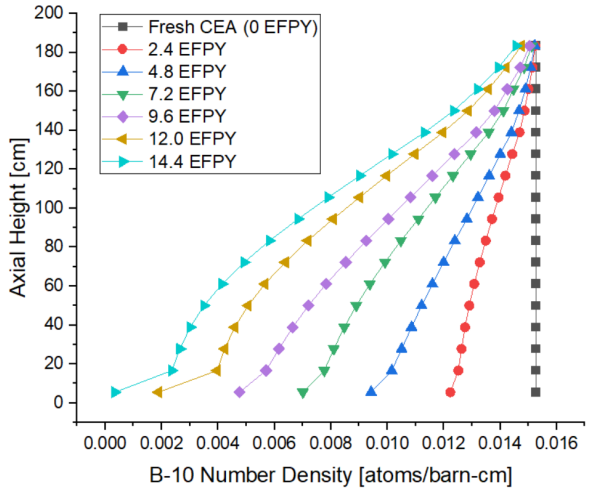

[B-10 Number Density in R4 Bank]

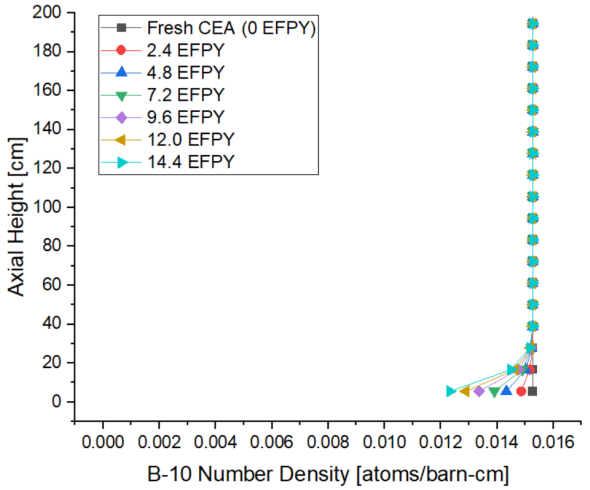

[B-10 Number Density in S2 Bank]

Thank you for your attention

Seoul National University
Monte Carlo Laboratory

A.1. N-1 Condition Search Results (1/2)

CEA Index	Reactivity at N-1 Condition (SD) [%Δρ]			
	HZP		CZP	
	Eq. Xe.	No. Xe.	Eq. Xe.	No. Xe.
ARI	-22.80(0.01)	-21.60(0.01)	-8.07(0.01)	-6.80(0.01)
A1	-18.67(0.01)	-17.43(0.01)	-4.30(0.00)	-2.99(0.00)
A2	-18.52(0.01)	-17.25(0.01)	-4.29(0.00)	-2.97(0.01)
A4	-20.71(0.01)	-19.56(0.01)	-6.24(0.00)	-5.00(0.00)
A5	-20.95(0.01)	-19.79(0.01)	-6.58(0.00)	-5.32(0.00)
A6	-18.43(0.01)	-17.29(0.01)	-4.14(0.00)	-2.94(0.00)
A7	-18.83(0.01)	-17.63(0.01)	-4.72(0.00)	-3.43(0.00)
A8	-18.47(0.01)	-17.22(0.00)	-4.17(0.00)	-2.87(0.00)
B2	-18.68(0.01)	-17.44(0.01)	-4.24(0.00)	-2.92(0.00)
B3	-20.37(0.01)	-19.17(0.01)	-5.85(0.00)	-4.55(0.00)
B4	-21.42(0.01)	-20.25(0.01)	-7.03(0.01)	-5.77(0.00)
B5	-20.17(0.01)	-18.97(0.01)	-5.70(0.00)	-4.43(0.00)
B7	-16.85(0.01)	-15.62(0.00)	-2.80(0.00)	-1.52(0.00)
C2	-21.88(0.01)	-20.68(0.01)	-7.36(0.01)	-6.08(0.00)
C3	-19.72(0.01)	-18.46(0.01)	-4.97(0.00)	-3.68(0.00)
C4	-20.94(0.01)	-19.76(0.01)	-6.45(0.00)	-5.15(0.00)
C5	-19.90(0.01)	-18.66(0.01)	-5.55(0.00)	-4.22(0.01)
C6	-17.08(0.00)	-15.83(0.01)	-2.94(0.00)	-1.63(0.00)
C7	-20.38(0.00)	-19.15(0.01)	-6.02(0.00)	-4.75(0.01)
D4	-19.39(0.01)	-18.10(0.01)	-4.70(0.00)	-3.39(0.00)
D5	-18.89(0.00)	-17.62(0.00)	-4.39(0.00)	-3.07(0.00)

[N-1 Condition Search Results at BOC]

CEA Index	Reactivity at N-1 Condition (SD) [%Δρ]			
	HZP		CZP	
	Eq. Xe.	No. Xe.	Eq. Xe.	No. Xe.
ARI	-23.32(0.01)	-22.20(0.01)	-8.71(0.00)	-7.49(0.01)
A1	-19.10(0.01)	-17.88(0.01)	-4.82(0.01)	-3.55(0.00)
A2	-19.06(0.01)	-17.88(0.01)	-4.96(0.00)	-3.71(0.00)
A4	-21.30(0.01)	-20.20(0.01)	-6.94(0.00)	-5.77(0.01)
A5	-21.53(0.01)	-20.42(0.01)	-7.25(0.00)	-6.06(0.00)
A6	-19.01(0.00)	-17.93(0.00)	-4.80(0.00)	-3.67(0.00)
A7	-19.35(0.01)	-18.20(0.01)	-5.36(0.00)	-4.13(0.00)
A8	-18.89(0.00)	-17.69(0.01)	-4.69(0.00)	-3.45(0.00)
B2	-19.19(0.00)	-18.00(0.01)	-4.84(0.00)	-3.60(0.00)
B3	-20.94(0.01)	-19.78(0.01)	-6.52(0.01)	-5.32(0.01)
B4	-21.98(0.01)	-20.84(0.01)	-7.66(0.01)	-6.51(0.00)
B5	-20.73(0.01)	-19.59(0.00)	-6.40(0.00)	-5.18(0.00)
B7	-17.39(0.01)	-16.21(0.01)	-3.43(0.00)	-2.20(0.00)
C2	-22.36(0.01)	-21.21(0.01)	-7.95(0.01)	-6.75(0.01)
C3	-20.21(0.01)	-19.03(0.01)	-5.54(0.00)	-4.31(0.01)
C4	-21.46(0.01)	-20.31(0.01)	-7.09(0.00)	-5.85(0.01)
C5	-20.43(0.01)	-19.25(0.01)	-6.19(0.01)	-4.92(0.00)
C6	-17.60(0.01)	-16.40(0.00)	-3.53(0.00)	-2.30(0.00)
C7	-20.86(0.01)	-19.70(0.00)	-6.62(0.01)	-5.39(0.00)
D4	-19.79(0.00)	-18.59(0.01)	-5.19(0.00)	-3.93(0.00)
D5	-19.31(0.01)	-18.09(0.01)	-4.90(0.00)	-3.64(0.00)

[N-1 Condition Search Results at IOC]

A.1. N-1 Condition Search Results (2/2)

CEA Index	Reactivity at N-1 Condition (SD) [%Δρ]			
	HZP		CZP	
	Eq. Xe.	No. Xe.	Eq. Xe.	No. Xe.
ARI	-25.36(0.01)	-24.21(0.01)	-11.28(0.01)	-10.07(0.00)
A1	-20.20(0.01)	-18.94(0.01)	-6.11(0.00)	-4.80(0.00)
A2	-20.31(0.01)	-19.01(0.00)	-7.23(0.00)	-5.89(0.00)
A4	-23.31(0.01)	-22.18(0.01)	-9.77(0.01)	-8.61(0.00)
A5	-23.54(0.01)	-22.41(0.01)	-10.06(0.00)	-8.88(0.00)
A6	-20.83(0.01)	-19.73(0.00)	-7.49(0.00)	-6.36(0.00)
A7	-20.71(0.00)	-19.46(0.00)	-7.61(0.00)	-6.33(0.00)
A8	-19.95(0.01)	-18.67(0.01)	-5.98(0.00)	-4.67(0.00)
B2	-20.45(0.01)	-19.17(0.01)	-6.79(0.00)	-5.47(0.00)
B3	-22.78(0.01)	-21.60(0.01)	-9.27(0.00)	-8.06(0.01)
B4	-24.00(0.01)	-22.90(0.02)	-10.36(0.00)	-9.22(0.00)
B5	-22.58(0.01)	-21.40(0.01)	-9.17(0.01)	-7.94(0.00)
B7	-18.42(0.01)	-17.12(0.01)	-5.35(0.00)	-4.05(0.00)
C2	-24.01(0.01)	-22.82(0.01)	-9.96(0.01)	-8.68(0.01)
C3	-21.48(0.01)	-20.20(0.01)	-7.35(0.00)	-6.05(0.00)
C4	-23.09(0.01)	-21.86(0.01)	-9.32(0.00)	-8.02(0.00)
C5	-21.93(0.01)	-20.66(0.01)	-8.47(0.00)	-7.15(0.00)
C6	-18.66(0.01)	-17.35(0.01)	-5.52(0.00)	-4.20(0.00)
C7	-22.18(0.01)	-20.93(0.01)	-8.48(0.00)	-7.22(0.00)
D4	-20.77(0.01)	-19.49(0.01)	-6.34(0.01)	-5.00(0.00)
D5	-20.37(0.01)	-19.11(0.00)	-6.18(0.00)	-4.85(0.00)

[N-1 Condition Search Results at MOC]

CEA Index	Reactivity at N-1 Condition (SD) [%Δρ]			
	HZP		CZP	
	Eq. Xe.	No. Xe.	Eq. Xe.	No. Xe.
ARI	-29.02(0.01)	-27.58(0.01)	-14.80(0.00)	-13.23(0.01)
A1	-24.96(0.01)	-23.55(0.01)	-9.95(0.00)	-8.49(0.00)
A2	-23.69(0.01)	-22.19(0.01)	-10.23(0.00)	-8.59(0.00)
A4	-25.74(0.01)	-24.17(0.01)	-12.55(0.00)	-10.85(0.00)
A5	-26.27(0.01)	-24.74(0.01)	-13.04(0.01)	-11.38(0.00)
A6	-23.15(0.01)	-21.59(0.01)	-10.10(0.00)	-8.42(0.00)
A7	-24.14(0.01)	-22.66(0.01)	-10.72(0.00)	-9.13(0.00)
A8	-24.57(0.01)	-23.17(0.01)	-9.72(0.00)	-8.24(0.00)
B2	-24.20(0.01)	-22.74(0.01)	-9.98(0.00)	-8.45(0.00)
B3	-25.51(0.01)	-23.97(0.01)	-12.07(0.00)	-10.38(0.00)
B4	-27.29(0.01)	-25.83(0.01)	-13.64(0.01)	-12.06(0.00)
B5	-25.17(0.01)	-23.63(0.01)	-11.88(0.00)	-10.22(0.00)
B7	-21.57(0.01)	-20.10(0.00)	-8.16(0.00)	-6.58(0.00)
C2	-28.05(0.01)	-26.64(0.01)	-13.53(0.01)	-12.06(0.00)
C3	-25.34(0.00)	-23.91(0.01)	-10.58(0.00)	-9.07(0.00)
C4	-27.02(0.01)	-25.58(0.01)	-12.81(0.00)	-11.24(0.00)
C5	-25.73(0.01)	-24.26(0.01)	-11.83(0.01)	-10.22(0.00)
C6	-21.95(0.01)	-20.50(0.00)	-8.41(0.00)	-6.84(0.00)
C7	-26.05(0.01)	-24.64(0.01)	-11.86(0.00)	-10.33(0.00)
D4	-25.65(0.01)	-24.27(0.00)	-10.16(0.00)	-8.70(0.00)
D5	-25.22(0.01)	-23.82(0.01)	-10.04(0.01)	-8.57(0.01)

[N-1 Condition Search Results at EOC]

A.2. Reactivity Coefficients (1/3)

- FTC
  - FTC is primarily driven by the Doppler broadening of U-238 resonance peaks, which is proportional to the square root of the absolute fuel temperature.
  - FTC is evaluated from isolate Doppler feedback by perturbing fuel temperature (In this study, +50K) while keeping moderator conditions constant.

$$\alpha_f = \frac{\Delta\rho_f}{\Delta\sqrt{\bar{T}f}}$$

- MTC including Density Effect
  - MTC is derived at HFP by simulating a power exchange (In this study, 129% power) to account for non-uniform axial temperature gradients.
  - MTC is evaluated from the total power defect by subtracting the Doppler contribution to isolate the moderator feedback.

$$\alpha_c = \frac{\Delta\rho_p - \alpha_f(\Delta\sqrt{\bar{T}_f})}{\Delta\bar{T}_c}$$

A.2. Reactivity Coefficients (2/3)

- Reactivity Coefficients * HFP and CRP Conditions
  - In the point kinetics model, only FTC*, the cross-section component of MTC, and MDC were applied.
  - In conventional pre-trip analyses, a more negative MTC is applied to maximize the positive reactivity insertion. Simultaneously, a less negative FTC is used to minimize the negative reactivity feedback.

-		BOC		IOC		MOC		EOC	
		Eq. Xe.	No Xe.	Eq. Xe.	No Xe.	Eq. Xe.	No Xe.	Eq. Xe.	No Xe.
Fuel Temperature Coefficient (FTC)	FTC (SD) [pcm/K]	-2.38 (0.09)	-2.33 (0.10)	-2.27 (0.11)	-2.41 (0.11)	-2.61 (0.10)	-2.65 (0.10)	-2.83 (0.10)	-2.81 (0.09)
	FTC* (SD) [pcm/$\sqrt{K}$]	-128.08 (4.99)	-125.25 (5.15)	-122.14 (5.77)	-129.90 (5.70)	-140.72 (5.65)	-142.57 (5.55)	-152.28 (5.21)	-151.13 (4.83)
Moderator Temperature Coefficient (MTC)	Cross-section Component of MTC (SD) [pcm/K]	-6.50 (0.09)	-6.35 (0.10)	-5.27 (0.12)	-5.75 (0.11)	-0.28 (0.10)	-0.88 (0.10)	2.04 (0.10)	1.12 (0.09)
	Moderator Density Coefficient (MDC) (SD) [pcm/(kg/m^3)]	35.61 (0.66)	32.78 (0.63)	30.09 (0.58)	33.27 (0.70)	36.76 (0.63)	36.41 (0.62)	53.99 (0.79)	47.33 (0.71)
	MTC (SD) [pcm/K]	-91.21 (1.58)	-86.75 (1.54)	-77.93 (1.39)	-86.62 (1.69)	-87.83 (1.50)	-90.05 (1.52)	-119.60 (1.79)	-108.95 (1.64)

* Appendix A.2. Calculation Methodology for Reactivity Coefficients

: Maximum : Minimum

A.2. Reactivity Coefficients (3/3)

- Reactivity Coefficients * HFP and CRP Conditions

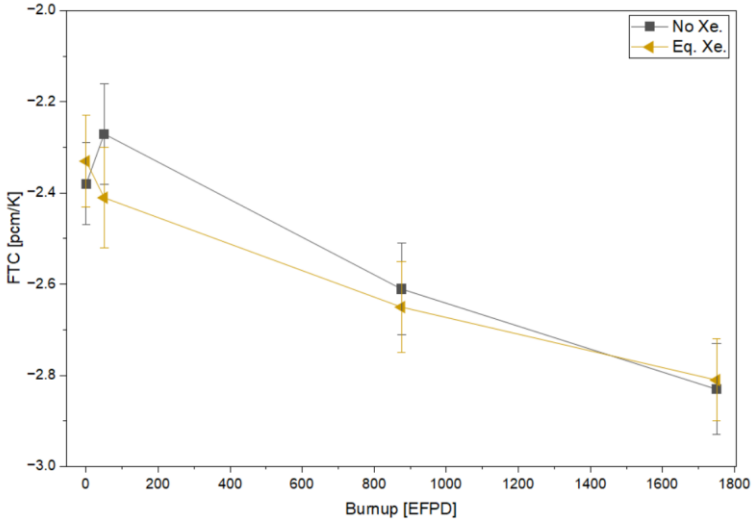

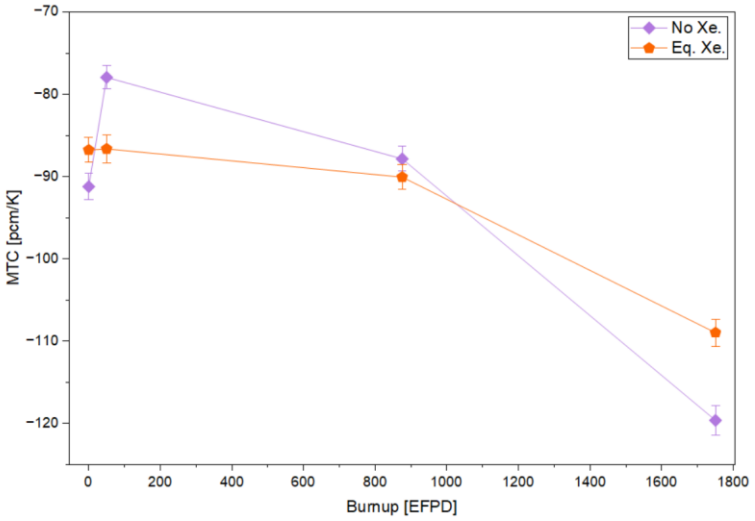

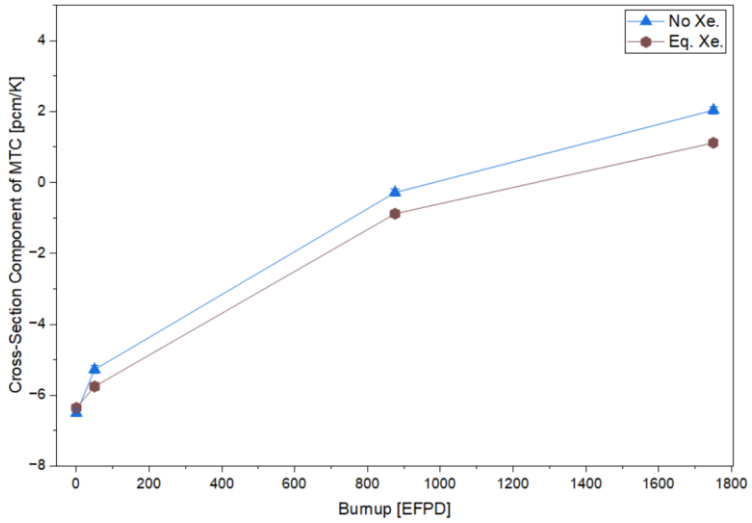

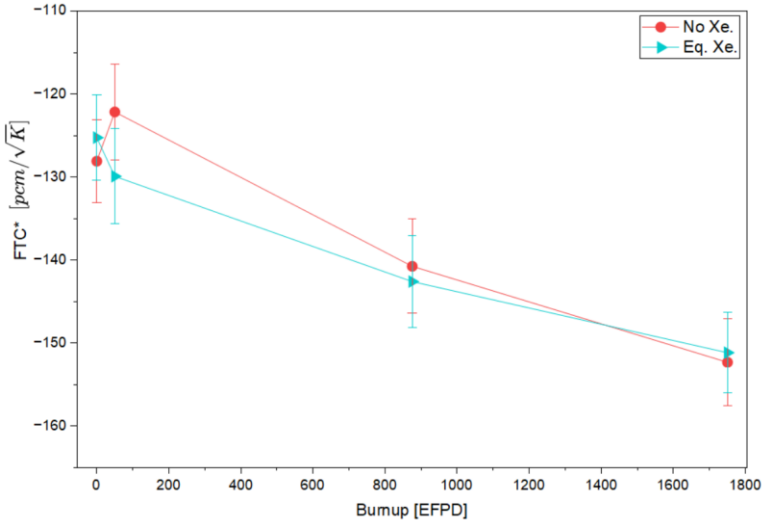

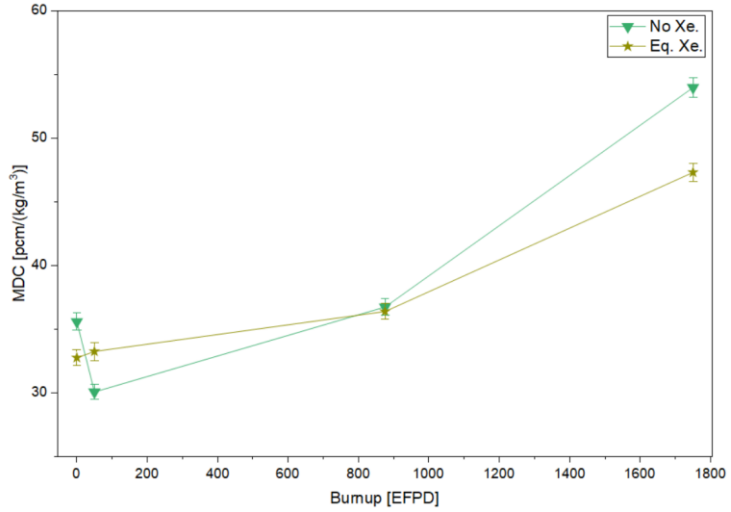

A.3. Kinetic Parameter (1/3)

- Kinetic Parameter * HFP and CRP Conditions
  - β_{eff} decreases toward EOC due to U-235 depletion and Pu-239 buildup.
  - The smaller β_{eff} accelerates the core's response to positive reactivity insertions.

-	BOC		IOC		MOC		EOC	
	Eq. Xe.	No Xe.	Eq. Xe.	No Xe.	Eq. Xe.	No Xe.	Eq. Xe.	No Xe.
β_{eff} (%RSD)	0.007078 (0.25)	0.007076 (0.22)	0.006872 (0.22)	0.006943 (0.18)	0.005834 (0.23)	0.005813 (0.24)	0.005306 (0.22)	0.005358 (0.27)
Λ (%RSD) [sec]	0.000016 (0.02)	0.000016 (0.03)	0.000016 (0.03)	0.000016 (0.03)	0.000018 (0.02)	0.000018 (0.02)	0.000021 (0.02)	0.000020 (0.02)

* The 6-group effective delayed neutron fractions and decay constants are provided in Appendix A.3.

: Maximum : Minimum

A.3. Kinetic Parameter (2/3)

- Kinetic Parameter * HFP and CRP Conditions

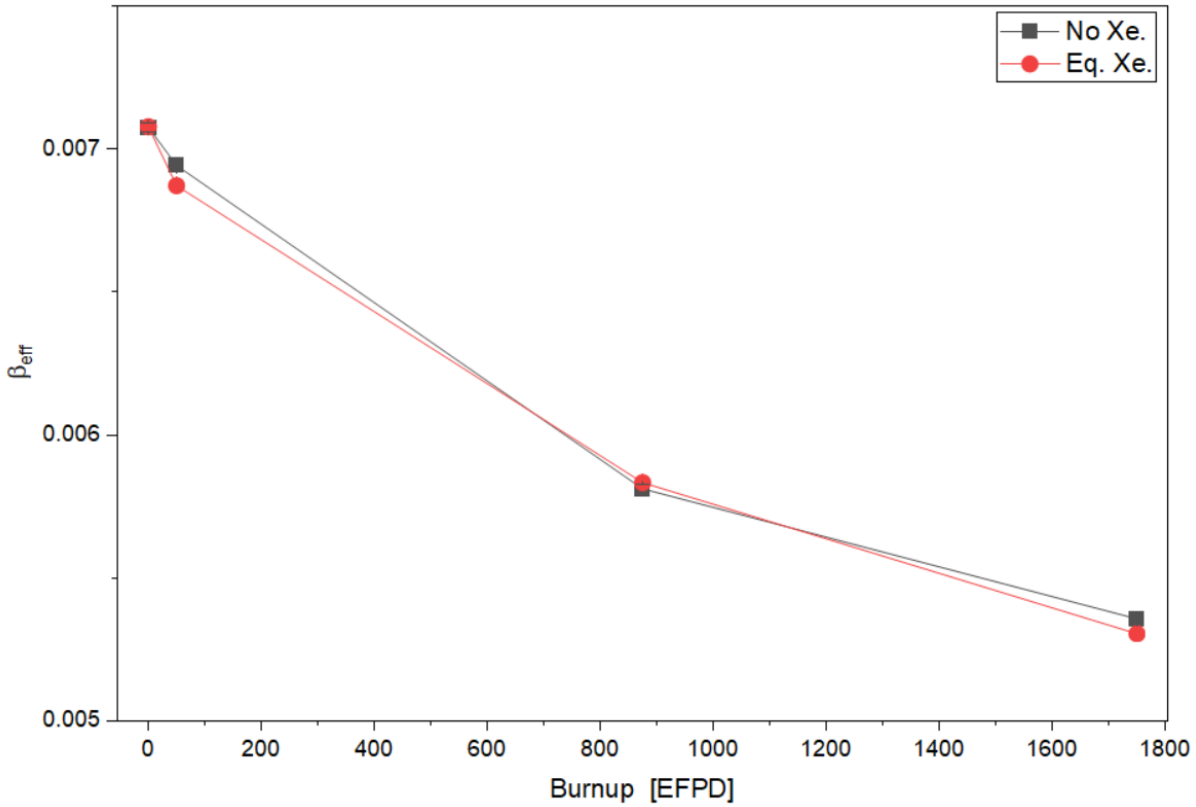

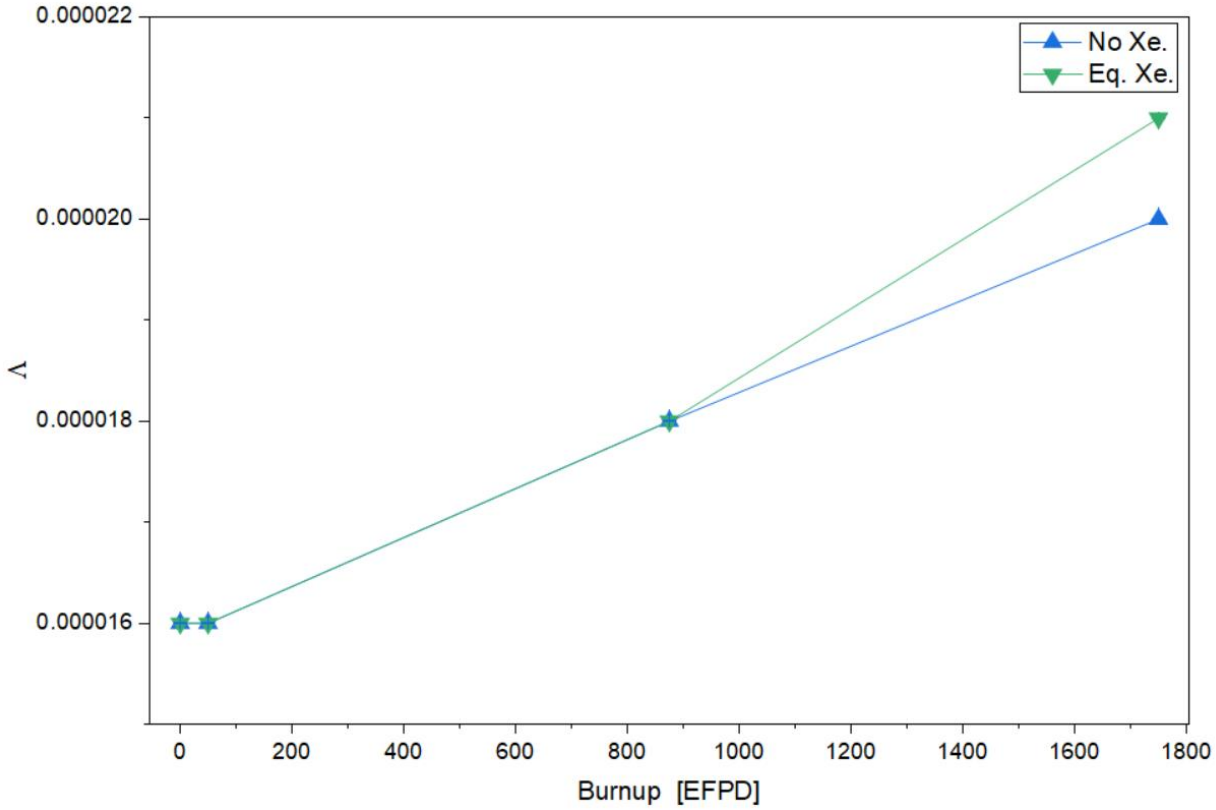

A.3. Kinetic Parameter (3/3)

-	Group	BOC		IOC		MOC		EOC	
		Eq. Xe.	No Xe.	Eq. Xe.	No Xe.	Eq. Xe.	No Xe.	Eq. Xe.	No Xe.
$\beta_{i,eff}$ (%RSD)	1	0.000223 (1.29)	0.000230 (1.30)	0.000217 (1.02)	0.000224 (1.17)	0.000177 (1.18)	0.000179 (1.56)	0.000155 (1.23)	0.000161 (1.20)
	2	0.001215 (0.49)	0.001206 (0.60)	0.001174 (0.62)	0.001188 (0.56)	0.001023 (0.54)	0.001012 (0.48)	0.000944 (0.57)	0.000958 (0.67)
	3	0.001174 (0.49)	0.001170 (0.45)	0.001151 (0.50)	0.001162 (0.52)	0.000967 (0.54)	0.000960 (0.61)	0.000864 (0.62)	0.000870 (0.65)
	4	0.002731 (0.38)	0.002741 (0.29)	0.002648 (0.38)	0.002662 (0.34)	0.002199 (0.31)	0.002200 (0.36)	0.001985 (0.38)	0.002007 (0.44)
	5	0.001220 (0.55)	0.001219 (0.46)	0.001194 (0.46)	0.001210 (0.57)	0.001047 (0.66)	0.001048 (0.62)	0.000975 (0.54)	0.000982 (0.64)
	6	0.000514 (0.80)	0.000509 (0.77)	0.000487 (0.94)	0.000497 (0.89)	0.000421 (0.92)	0.000414 (0.71)	0.000383 (0.61)	0.000381 (0.84)
λ_i (%RSD)	1	0.013357 (0.00)	0.013357 (0.00)	0.013355 (0.00)	0.013355 (0.00)	0.013346 (0.00)	0.013346 (0.00)	0.013348 (0.00)	0.013348 (0.00)
	2	0.032640 (0.00)	0.032640 (0.00)	0.032588 (0.00)	0.032587 (0.00)	0.032051 (0.00)	0.032027 (0.00)	0.031707 (0.00)	0.031750 (0.00)
	3	0.120961 (0.00)	0.120961 (0.00)	0.120756 (0.00)	0.120750 (0.00)	0.118829 (0.00)	0.118751 (0.00)	0.117826 (0.00)	0.117948 (0.00)
	4	0.304262 (0.00)	0.304259 (0.00)	0.303978 (0.00)	0.303969 (0.00)	0.301593 (0.00)	0.301507 (0.00)	0.300665 (0.00)	0.300773 (0.00)
	5	0.853485 (0.00)	0.853477 (0.00)	0.853706 (0.00)	0.853708 (0.00)	0.856209 (0.00)	0.856320 (0.00)	0.857791 (0.00)	0.857596 (0.00)
	6	2.866842 (0.00)	2.866815 (0.00)	2.863446 (0.00)	2.863341 (0.00)	2.837882 (0.00)	2.837129 (0.00)	2.832177 (0.00)	2.832698 (0.00)

A.4. SCRAM Worth (1/3)

- SCRAM Worth * HFP and CRP Conditions
  - For a conservative analysis, the SCRAM worth evaluated at 100% power was used in the analysis.

-		BOC		IOC		MOC		EOC	
		Eq. Xe.	No Xe.	Eq. Xe.	No Xe.	Eq. Xe.	No Xe.	Eq. Xe.	No Xe.
SCRAM Worth[1] [%Δρ]	100% Power	19.92	19.19	20.58	19.53	21.78	20.96	25.69	24.61
	105% Power	19.96	19.27	20.66	19.60	21.87	21.06	25.80	24.78
	115% Power	20.09	19.42	20.84	19.72	22.00	21.22	26.05	25.08
	125% Power	20.21	19.56	21.00	19.87	22.17	21.41	26.30	25.42
AO		-0.25	-0.50	-0.35	-0.44	-0.26	-0.50	0.18	-0.07

1) $\Delta\rho_{\mathrm{SCRAM}} = \rho_{\mathrm{HFP,\,CRP}} - \rho_{\mathrm{HFP,\,N-1}}$

: Maximum : Minimum

A.4. SCRAM Worth (2/3)

- SCRAM Worth * HFP and CRP Conditions

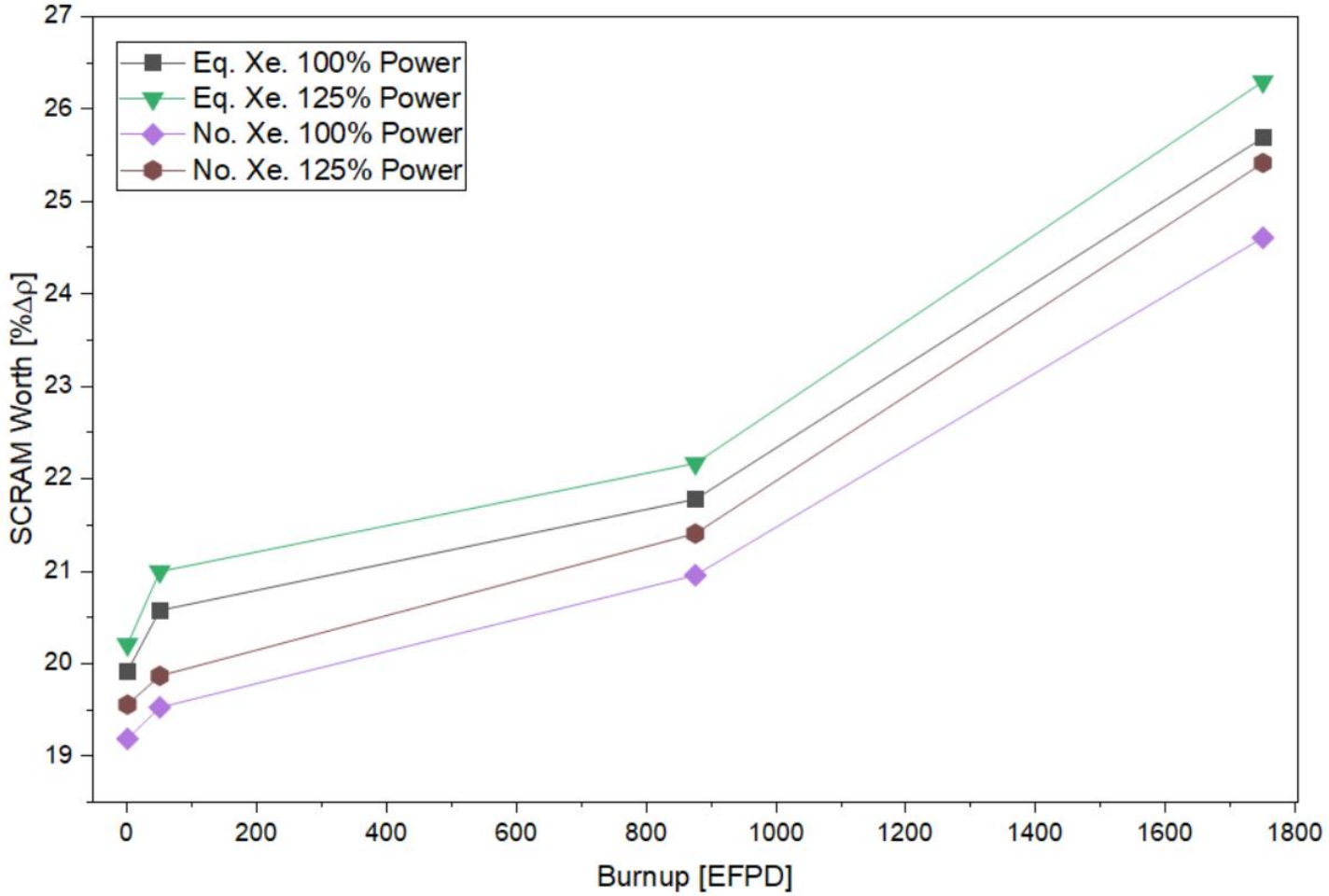

A.4. SCRAM Worth (3/3)

- Axial Power Distribution

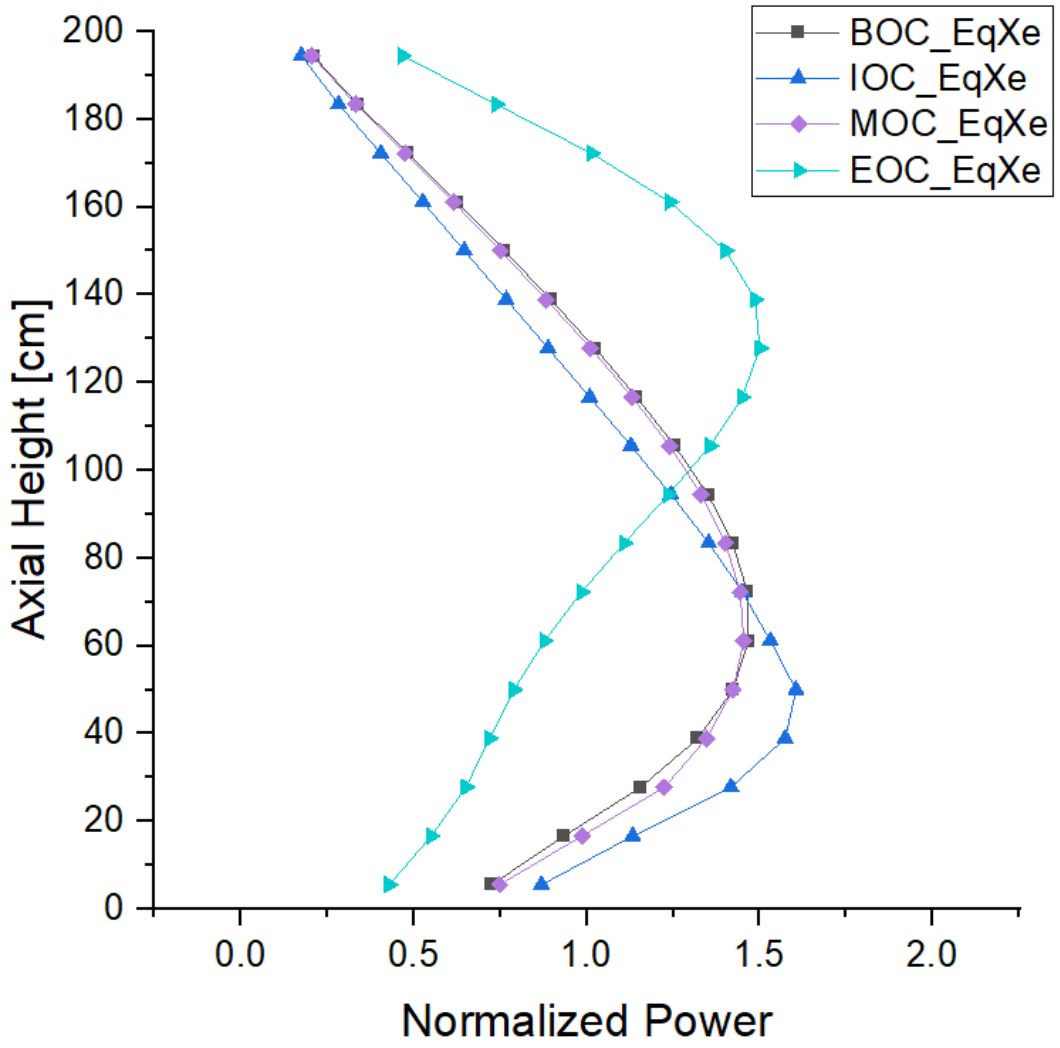

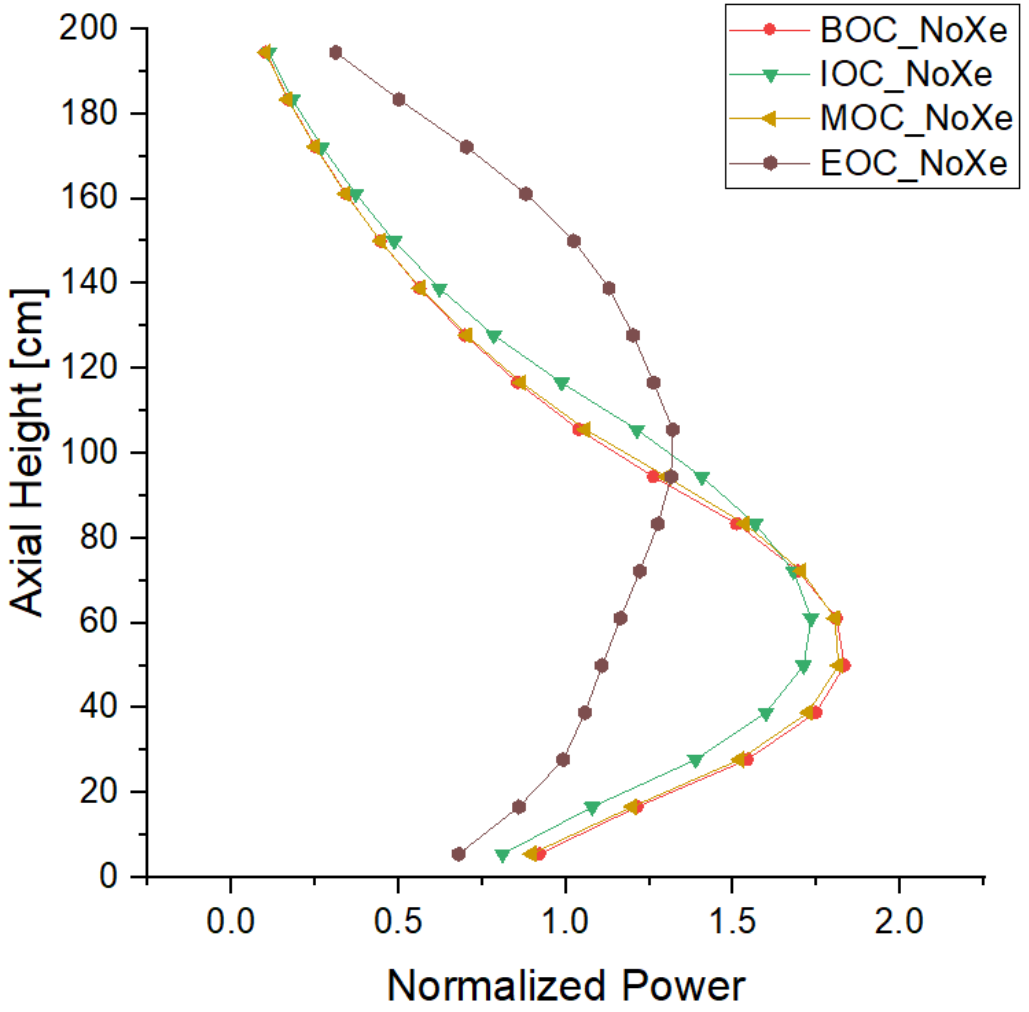

A.5. Point Kinetics Feedback Model (1/3)

The thermal-hydraulic feedback in the Point Kinetics Model is evaluated based on the energy balance within the reactor core.

$$\bar{T}_o = T_i + \frac{1}{W c_p} P \quad \text{— Eq. (1)}$$

where:

- T_i is the core inlet coolant temperature
- $\bar{T}_o$ is the core outlet coolant temperature averaged over the cross-sectional area of the core
- $\bar{T}_c$ is the coolant temperature averaged over the total volume of the coolant in active core
- W is the core mass flow rate in kg/s
- c_p is the coolant specific heat at constant pressure in J/kg-K

In a conventional large PWR, assuming a symmetric axial power distribution, the average coolant temperature is approximated as:

$$\bar{T}_c = \frac{1}{2}(T_i + \bar{T}_o) \quad \text{— Eq. (2)}$$

Using this approximation, we can substitute Eq. (1) to obtain the average coolant temperature in terms of the known inlet coolant temperature and the thermal power:

$$\bar{T}_c = T_i + \frac{1}{2W c_p} P \quad \text{— Eq. (3)}$$

A.5. Point Kinetics Feedback Model (2/3)

However, the SBF core typically exhibits a bottom-skewed axial power distribution and varying AO depending on the burnup. To account for these diverse power distributions, an axial shape factor f_z is introduced:

$$\bar{T}_c = T_i + \frac{f_z}{W c_p} P \quad \text{— Eq. (4)}$$

Consequently, the coupled energy balance equations for the coolant and fuel are expressed as follows:

$$M_c c_p \frac{d}{dt} \bar{T}_c(t) = \frac{1}{R_f} \left[\bar{T}_f(t) - \bar{T}_c(t)\right] - \frac{1}{f_z} W c_p [\bar{T}_c - T_i] \quad \text{— Eq. (5)}$$

Additionally, the average fuel temperature can be derived as:

$$M_f c_f \frac{d}{dt} \bar{T}_f(t) = P(t) - \frac{1}{R_f} [\bar{T}_f(t) - \bar{T}_c(t)] \quad \text{— Eq. (6)}$$

where:
For the fuel specific heat (c_f), the standard APR1400 temperature-dependent correlation is utilized.

The thermal resistance (R_f) is evaluated as a constant value and back-calculated from PRAGMA steady-state results for each specific burnup and Xenon condition to represent 3D core characteristics within the point model.

To represent 3D core characteristics within the point model, the axial shape factor (f_z) and coolant specific heat (c_p) are determined via interpolation from pre-calculated tables. These tables were generated using PRAGMA 3D core analysis across a range of inlet moderator temperatures (280˚C to 290˚C) and power levels (100% to 160%).

A.5. Point Kinetics Feedback Model (3/3)

The decay heat is applied as a constant fraction of the total power. This simplification is justified by the short time scale of the pre-trip analysis (< 7 sec), during which the change in decay heat is negligible.

Burnup	BOC	IOC	MOC	EOC
Decay Heat Fraction (P_{Decay}/P_{Total}) [%]	-	6.31	6.13	6.08

The core mass flow rate during the RCP coastdown is modeled using an inertia-based decay function, where the flow reduction rate is governed by the RCP coastdown coefficient (α).

$$W(t) = \frac{W_{trip}}{1 + \alpha\left(t - t_{trip}\right)} \quad \text{— Eq. (7)}$$

The system pressure is tracked by modeling the pressurizer steam space as an adiabatic system with conserved mass and energy.

$$V_{st}(t) = V_{total} - \frac{M_{liq.}}{\rho_{coolant}(t)} \quad \text{— Eq. (8)}$$

$$v\left(P, h_{st,0}\right) = \frac{V_{st}(t)}{m_{st,0}} \quad \text{— Eq. (9)}$$

$$P_{sys}(t) = \max\left(P_{calc}(t), P_{sat}\left(T_{avg}\right)\right) \quad \text{— Eq. (10)}$$

A.6. Transient Analysis over Time (1/7)

- Core Power. vs. Time

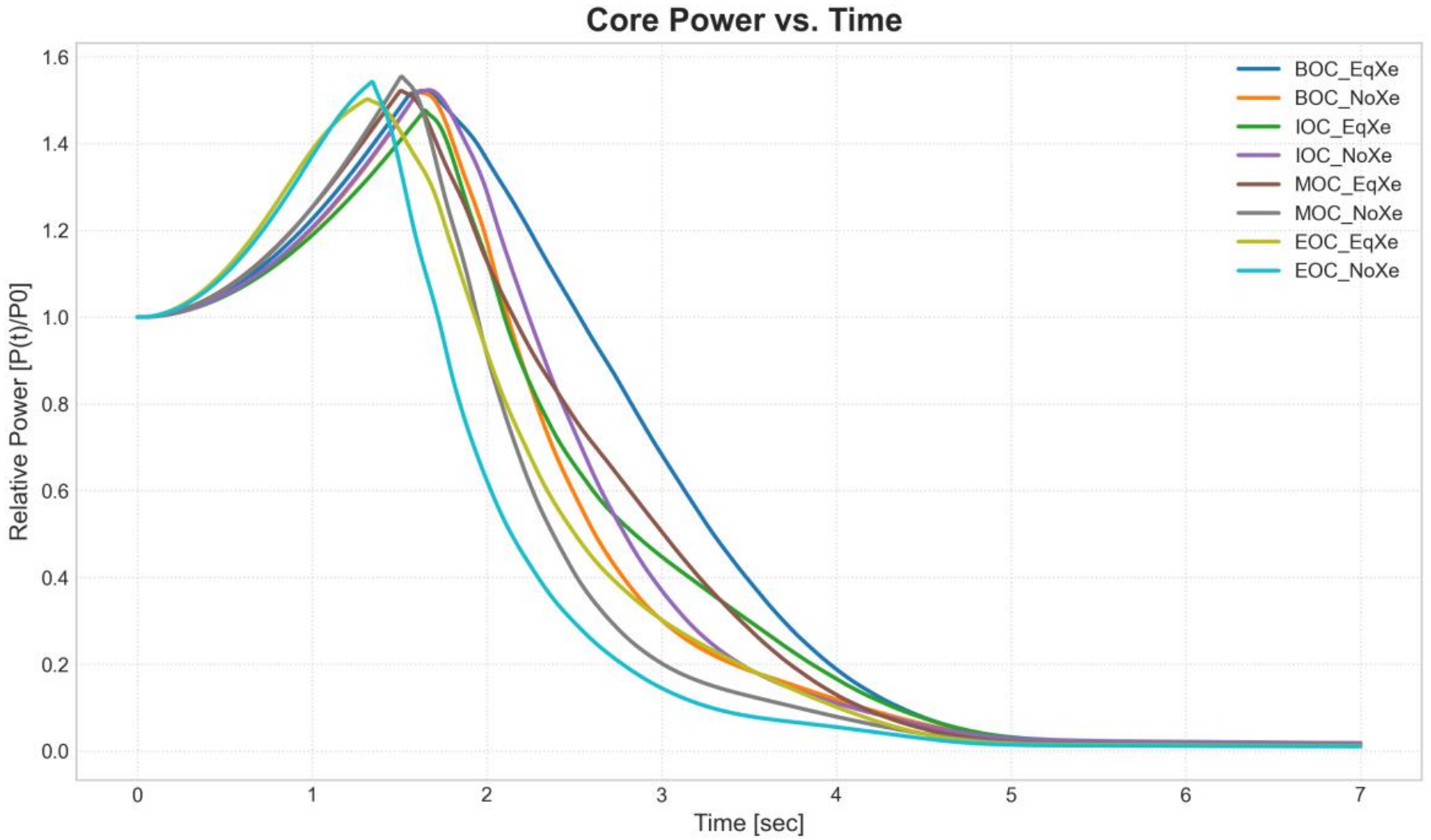

A.6. Transient Analysis over Time (2/7)

- Mass Flow Rate vs. Time

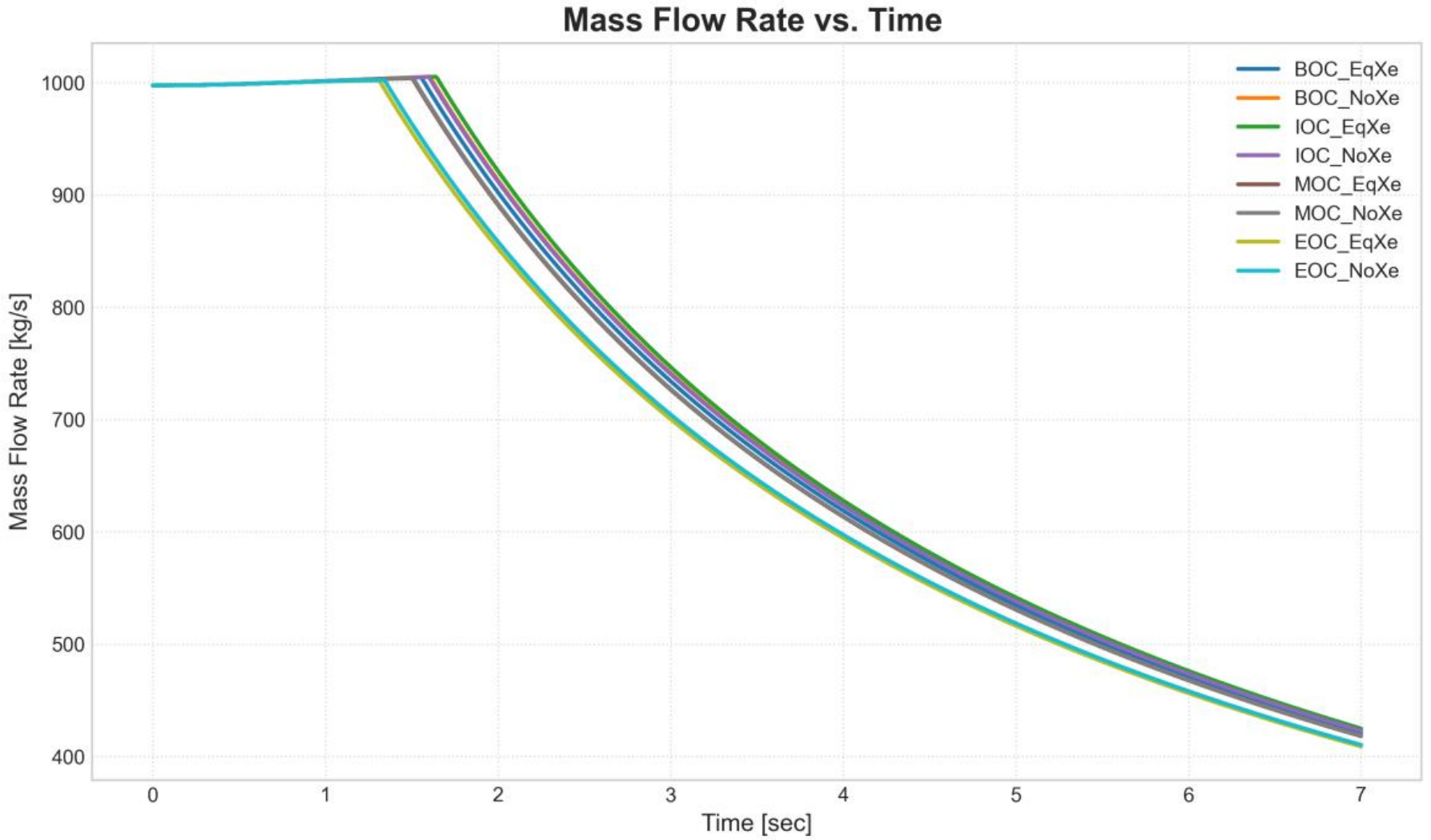

A.6. Transient Analysis over Time (3/7)

- RCS Pressure vs. Time

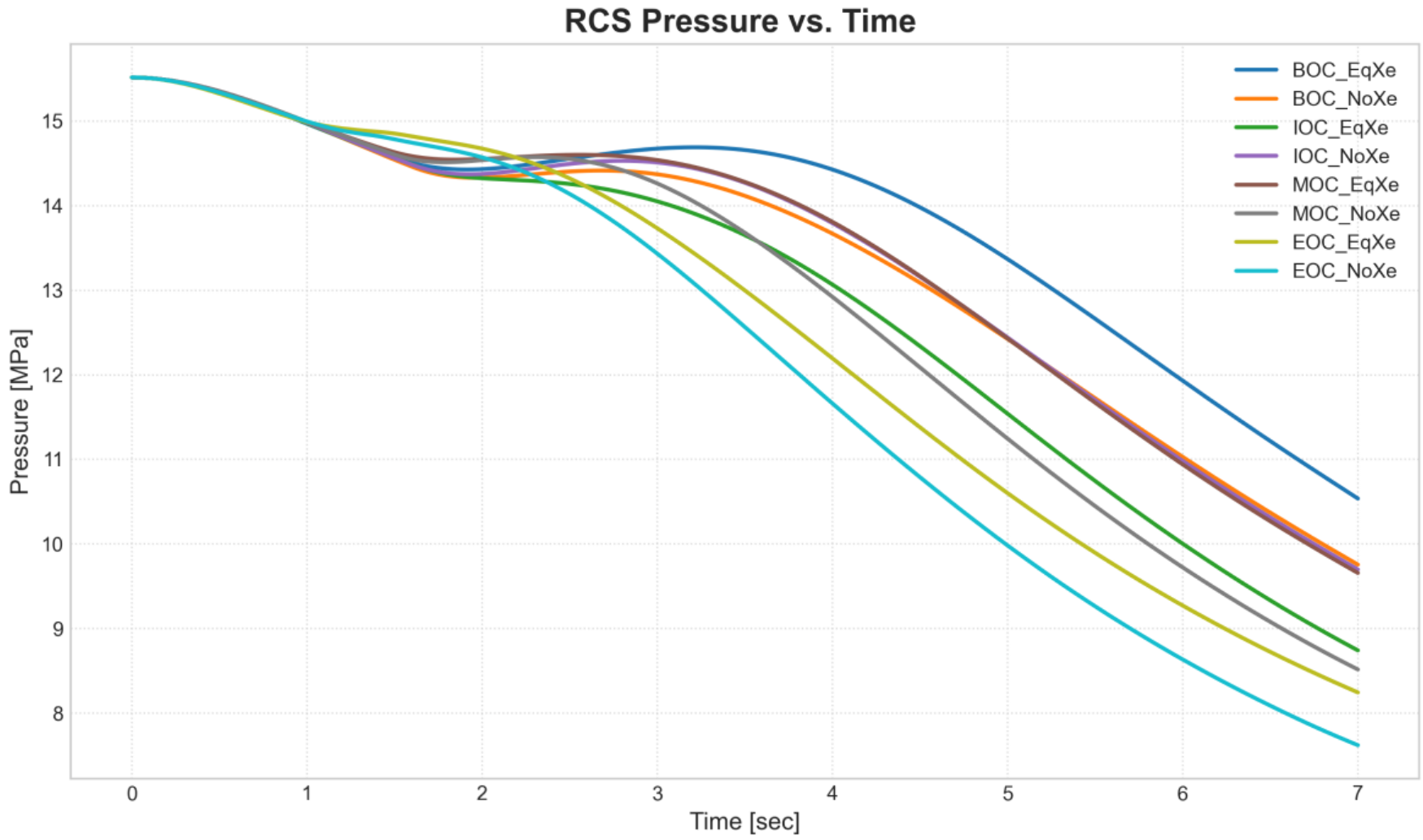

A.6. Transient Analysis over Time (4/7)

- Average Moderator Temp. vs. Time

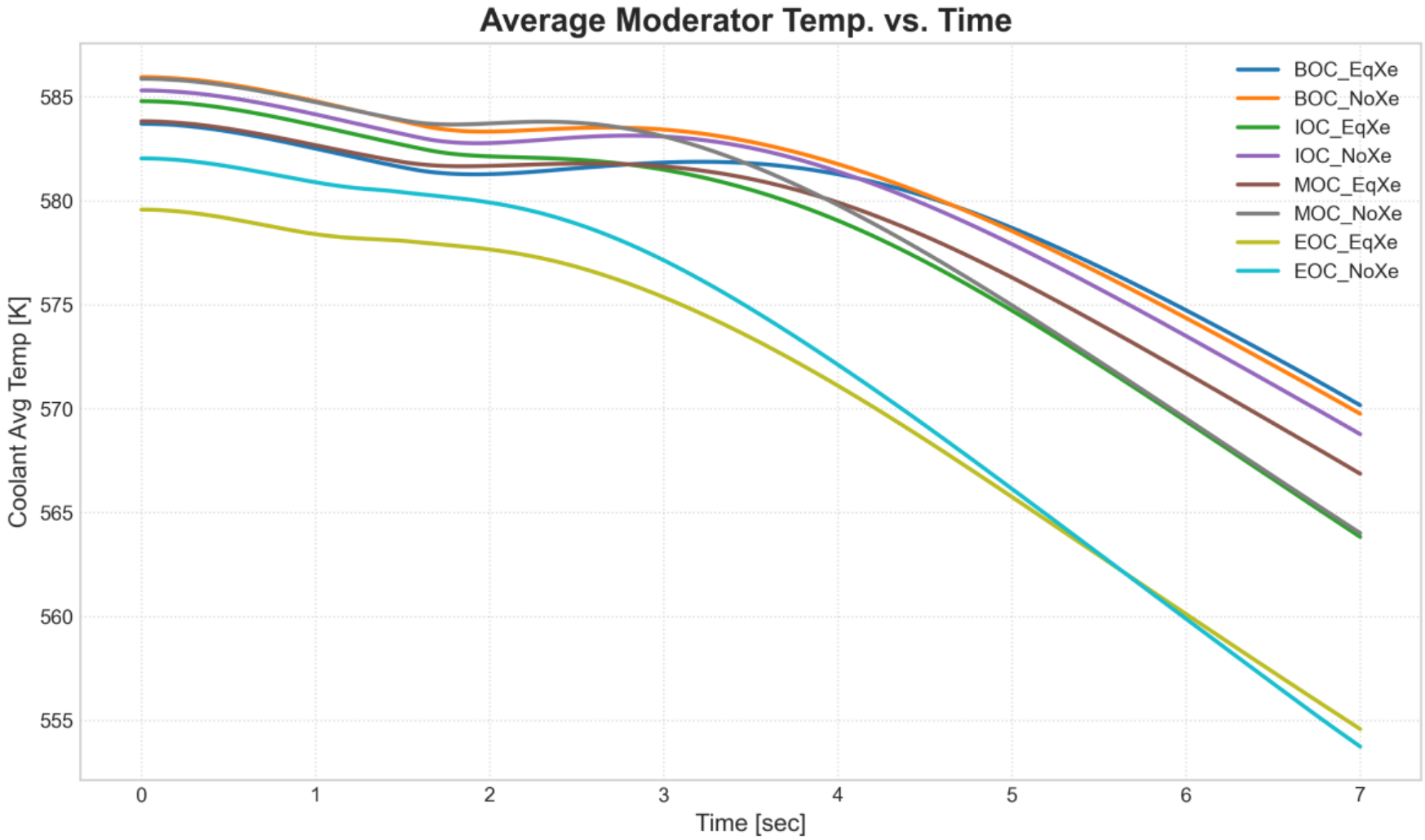

A.6. Transient Analysis over Time (5/7)

- Average Fuel Temp. vs. Time

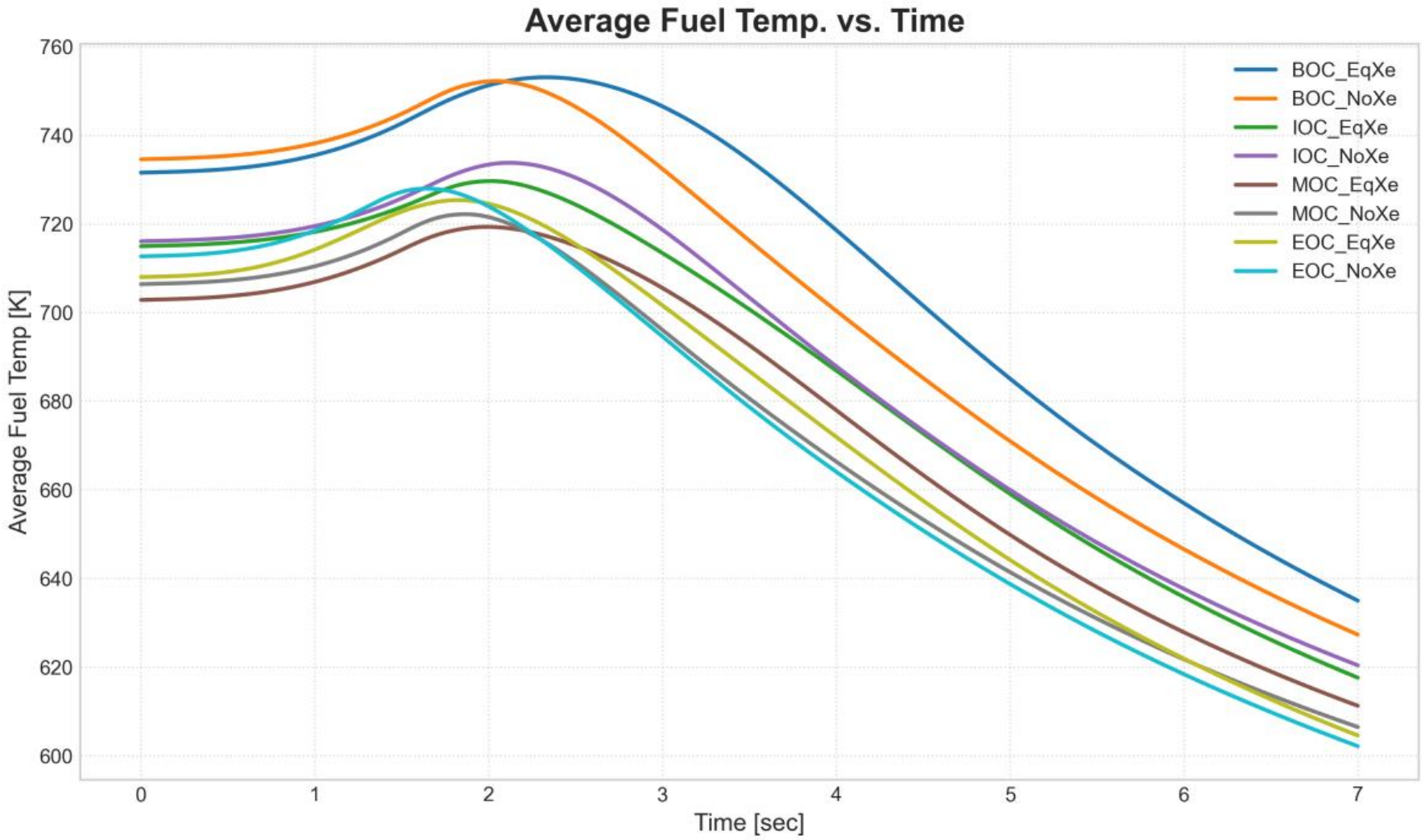

A.6. Transient Analysis over Time (6/7)

- Total Reactivity vs. Time

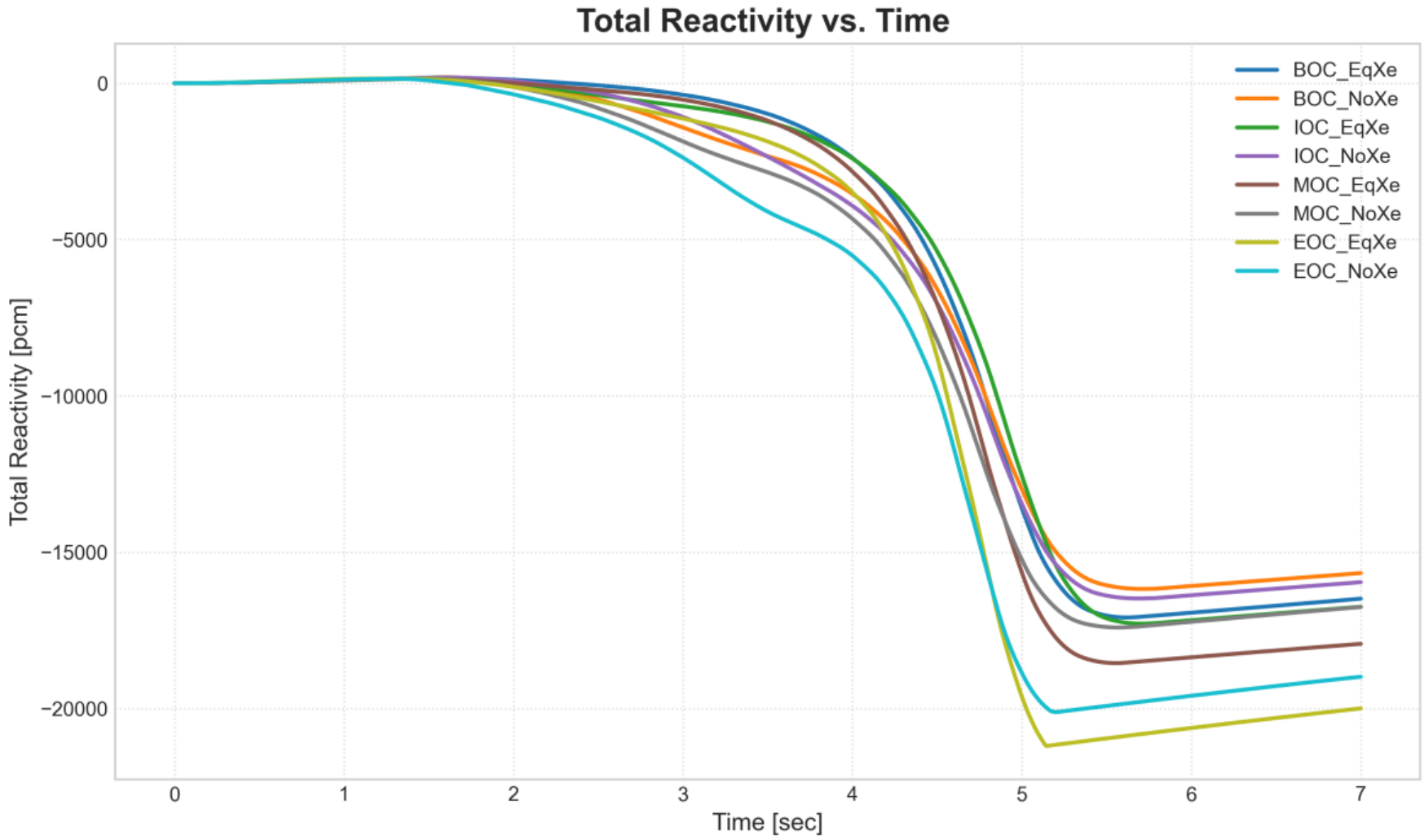

A.6. Transient Analysis over Time (7/7)

- Reactivity Behavior vs. Time (MOC, No Xe.)